**International Journal of Sustainable Energy and Environmental Research**
*2019 Vol. 8, No. 1, pp. 70-99*
*ISSN(e): 2306-6253*
*ISSN(p): 2312-5764*
*DOI: 10.18488/journal.13.2019.81.70.99*


# MODELLING AND SIMULATION OF PV SOLAR-THERMOELECTRIC GENERATORS USING NANO FLUIDS

**S. Sami**[1+]
**E. Marin**[2]

[1]*Research Center for Renewable Energy Catholic University of Cuenca, Cuenca, Ecuador & TransPacific Energy, Inc, NV, 89183, US.*
*Email: dr.ssami@transpacenergy.com*
[2]*Research Center for Renewable Energy Catholic University of Cuenca, Cuenca, Ecuador.*
*Email: edwinmarinesmc@gmail.com*

*(+ Corresponding author)*

**Article History**
Received: 22 January 2019
Revised: 27 February 2019
Accepted: 4 March 2019
Published: 9 May 2019

**Keywords**
PV-thermal panels
Thermoelectric generator
Nanofluids
Dynamic thermal behavior
Numerical model
Simulation
Validation.

## ABSTRACT

A simulation model has been developed to predict the behavior of a hybrid system composed of PV-Thermal panel and thermoelectric generator using nanofluids. The model has been established after the energy and mass conservation equations for nanofluids flow the dynamic behavior of the PV-Thermal panels, and the thermoelectric generator has been studied and analyzed under different nanofluid particles concentrations and different solar radiations conditions. The model fairly compared with existing data.

**Contribution/Originality:** Our contribution is to develop an original numerical model to predict the behavior of PV-Thermal and thermoelectric generator using nanofluids. The use of nanofluids shows significant improvements in the behavior of PV-Thermal and thermoelectric generator over the base fluid water. Our work uses different well-known nanofluids with various concentrations. This work represents a step forward in advancing the use of PV solar panels and thermoelectric generators. Our paper provides useful significant guidelines for the designers to use an integrated hybrid system of PV-Thermal and thermoelectric generators.

## 1. INTRODUCTION

Thermoelectric generators (TEG) are devices that convert temperature differences into electricity and thermal heat. TEGs are composed of several thermoelectric modules which are solid-state integrated circuits. These devices are established after the well-established thermoelectric well-known effects; the Peltier, Seebeck and Thomson effects (History, 1920; Buist, 1995; CRC, 1995; De Baetselier *et al.*, 1995a; De Baetselier *et al.*, 1995b; DiSalvo, 1999; Dziurdzia and Kos, 1999; Rowe, 1999; Dziurdzia and Kos, 2000; Snyder and Ursell, 2003; Dalola *et al.*, 2008; Jeffrey and Eric, 2008; Chen *et al.*, 2009; Freunek *et al.*, 2009; Beeby and White, 2010; Patrizia *et al.*, 2011; Faruk *et al.*, 2013; Piotr, 2014; Hashim *et al.*, 2016; Jatin *et al.*, 2016; The Science of Thermoelectric Materials, 2019; Warren, 2019). TEGs are driven by heat source as an energy driver such as gas or oil flame, stove, campfire, industrial machinery, furnace, electricity and solar energy. PV Solar panels convert solar radiations into usable electricity and can generate maximum rated power depending upon the intensity of solar radiation.

There is a significant number of parameters that must be considered in mathematical and simulation modeling of TEGs related to the thermoelectric materials, solid-state integrated circuits and modules. In addition, as previously mentioned the simulation model must include the module's effective Seebeck coefficient (SM), Electrical Resistance (RM), and Thermal Conductance (KM).

During the past several years, thermoelectric devices have attracted increasing attention as a 'green' and flexible source of electricity able to meet a wide range of power requirements. The results of a recent investigation by Rowe (1999) of the performance of thermoelectric generating systems powered by waste hot water indicated that electrical power can be produced by this method and at a price competitive with conventional utilities. Rowe also provided an overview of environmentally friendly applications of thermoelectric generation and assessed its potential as an alternative source of electrical power.

Reference (Faruk *et al.*, 2013) compared solar panels with TEGs. The comparative study dealt with different parameters such as efficiency, power generation capability and capacity, cost, size, potential consumer applications, and system installation complexity to generate power. In the study reported by reference (Faruk *et al.*, 2013) two separate laboratory environments were created to measure the power outputs and efficiencies. Both devices were tested at different locations due to different operating environmental conditions. A solar PV module was tested under sun-light whereas TEG module was tested inside an air conditioner condenser unit on the same days. Reference (Faruk *et al.*, 2013) presented test results of the comparison between the two energy generating systems and discussed potential applications.

Furthermore, Piotr (2014) study showed the viability of modelling of complex phenomena occurring in thermoelectric devices and coupled simulations of both thermal and electrical processes by means of electronic circuits simulators. Among others Pitor built-in procedures for solving differential and nonlinear equations, the electronic circuit SPICE-like simulators which can be used for simulation of other electrical phenomena. SPICE provided a reliable electrothermal model for the Peltier module. The energy conversion and distribution flow can be simulated in an autonomous sensor node.

Reference (Freunek *et al.*, 2009) described a new analytical physical model for thermoelectric generators (TEGs). The model includes the Thomson effect, the Peltier heat, a parameterization of the Joule heat, as well as all thermal and electrical resistances. Geometry optimization and investigations of the influence of Peltier heat and the heat source, as well as heat sink conditions and the load resistance, which affect the output power, are presented. The results are compared with measurements of commercially available thermoelectric generators and the fundamental thermodynamic limit. A comparison between the generators was also performed and presented.

More recently, a model for geometry optimization of thermoelectric devices in a hybrid photovoltaic - thermoelectric (PV/TE) system was presented by Hashim *et al.* (2016). It was claimed that the model can be used to determine the optimal geometry of thermoelectric modules at which the maximum power output is achieved. The results of simulation using the model showed that an increase in both the overall power output and conversion efficiency can be achieved by incorporating a thermoelectric generator (TEG) for waste heat recovery from photovoltaic cell. In addition, the results presented by this reference demonstrated that the geometry optimisation also needs to consider the "trade-off" between achieving a large power output and minimising the consumption of thermoelectric materials.

Currently, researchers are continually to improve the efficiency of photovoltaic technology. The most advanced and efficient solar cells are being developed, however, they are not yet available to the general public. To improve the efficiency of photovoltaics' (PV), references (Faragali *et al.*, 2008; Pei *et al.*, 2011; Good *et al.*, 2015; Liang *et al.*, 2015; Sami and Marin, 2017; Sami and Marin, 2017; Sami and Rivera, 2017; Sami, 2018; Sami, 2018; Sami and Campoverde, 2018; Sami and Marin, 2018) developed and implemented novel concepts of combined photovoltaic-thermal solar panel.

Significant research has been reported in the literature on nanofluid (Brenner *et al.*, 1993; Choi, 1995; Azo Material, 2004; Kakaç and Pramuanjaroenkij, 2009; Taylor *et al.*, 2011; Bachock and Pop, 2012; Saleh, 2012; Khullar *et al.*, 2013; Chaudhari and Walke, 2014; Nerella *et al.*, 2014; Allen, 2015; Kasaeian *et al.*, 2015; Sagadevan, 2015; Sharma *et al.*, 2017; Sami, 2018). Choi (1995) defined the nanofluid as suspensions of nano-sized particles. Knowing thermal properties of nanofluids are essential to understand their thermal behavior. Taylor *et al.* (2011) investigated theoretically and experimentally the nanofluids behavior utilizing power tower solar collectors Enhancement in the efficiency was observed and compared to the base fluid. Furthermore, Khullar *et al.* (2013) studied the enhancement of solar irradiance absorption capacity of nanofluid-based concentrating parabolic solar collectors, theoretically and compared the results with experimental data. The results of his study demonstrated an increase of 5-10 %.

More recently (Sami, 2018; Sami, 2018) presented a study, on the thermal characteristic's nano particles AI2O3, CuO, Fe304 and SiO2 circulating underneath a PV panel and thermal tank. During the course of the study, Reference (Sami, 2018) presented, a model to analyze the characteristics of the nanofluids fluid flow and compared the model's prediction to data published in the literature. He showed an increase of the efficiency of the PV-Th systems.

In this paper, a mathematical model is presented hereby to describe the heat and mass balances of the nanofluids flow that absorbs the excess heat released from the PV-Th solar panels and drives the thermoelectric generator modules. The model has been established after the energy and mass conservation equations coupled with the heat transfer equations of the nanofluids. The results of a behavior of the different nanofluids in PV-Th solar panel and thermoelectric generator are discussed. In addition, the simulated results are compared with available data. This model is intended to predict the behavior of integrated thermoelectric generator, and PV-TH under different operating conditions such as solar radiations, nanofluid flow rates, ambient temperatures, different PV cell temperatures and various volumetric nanofluid concentrations.

## 2. MATHEMATICAL MODEL

A schematic diagram of the integrated thermoelectric generator, and PV-Th solar hybrid system is shown in Figure 1. The system has a PV-Th collector, thermoelectric generator and monitoring system. The thermal tank was equipped with a heat exchanger to supply the heat for domestic or industrial use. In the hybrid system, the thin parallel tubes collectors are welded on the backside of photovoltaic solar panel for the circulation of the heat transfer cooling nanofluid. The flow thin tubes are in direct contact with the PV solar panel to ensure good heat transfer. The flow in each tube has different elements to permit the finite-difference formulation and analysis of the flow. It is assumed in the model that; the nanofluid is homogeneous, isotropic, incompressible, Newtonian, and inlet velocity and inlet temperature are constant, and also thermophysical properties of the nanofluids are constant. In the following, the conservation mass and energy equations are written and presented for nanofluids.

### *2.1. Solar PV MODEL*

The solar photovoltaic panel is constructed of various modules and each module is consisted of arrays and cells. The dynamic current output can be obtained as follows (Faragali *et al.*, 2008; Pei *et al.*, 2011; Good *et al.*, 2015; Liang *et al.*, 2015; Sami and Marin, 2017; Sami and Marin, 2017; Sami and Rivera, 2017; Sami, 2018; Sami and Campoverde, 2018).

$$I_P = I_L - I_o\left[\exp\left(\frac{q(V+I_PR_S)}{AkT_C} - \frac{V+I_PR_S}{R_{sh}}\right)\right] \quad (1)$$

$I_p$: Output current of the PV module

$I_L$ : Light generated current per module

$I_o$ : Reverse saturation current per module

V : Terminal voltage per module

$R_s$ : Diode series resistance per module

$R_{sh}$ : Diode shunt resistance per module

q: Electric charge

k : The Boltzman constant

A : Diode ideality factor for the module

The PV cell temperature, Tc, in Equation 1 is influenced by various factors such as solar radiations, ambient conditions, and wind speed. It is well known that the cell temperature impacts the PV output current, and performance, and its time-variation can be determined from references (Faragali *et al.*, 2008; Pei *et al.*, 2011; Good *et al.*, 2015; Liang *et al.*, 2015; Sami and Marin, 2017; Sami and Marin, 2017; Sami and Rivera, 2017; Sami, 2018; Sami, 2018; Sami and Campoverde, 2018; Sami and Marin, 2018). The AC power of the inverter output P(t) is calculated using the inverter efficiency $\eta_{inv}$ , output voltage between phases, neutral $V_{fn}$, and for single-phase current, $I_o$ and the power factor, $cos\phi$ as follows in Equation 2;

$$P(t) = \sqrt{3}\eta_{inv}V_{fn}I_o cos\phi \tag{2}$$

*2.2. PV Thermal Model*

It is assumed in this model that all PV cells behave the same; therefore, this model can be applied to the whole PV solar panel. This model is an extension of the work presented by Sami and Campoverde (2018); Sami (2018). The thermal heat absorbed by the PV solar cell can be calculated by the following equation (Faragali *et al.*, 2008; Pei *et al.*, 2011; Good *et al.*, 2015; Liang *et al.*, 2015; Sami and Marin, 2017; Sami and Marin, 2017; Sami and Rivera, 2017; Sami, 2018; Sami and Campoverde, 2018).

$$Q_{in} = \alpha_{abs} G S_p \tag{3}$$

Where;

$\alpha_{abs}$: Overall absorption coefficient

G: Total Solar radiation incident on the PV module

$S_p$: Total area of the PV module

Meanwhile, the PV cell Temperature is computed from the following heat balance (Faragali *et al.*, 2008; Kasaeian *et al.*, 2015).

$$mC_{p\_module}\frac{dT_C}{dt} = Q_{in} - Q_{conv} - Q_{elect} \tag{4}$$

Where;

$T_C$: PV Cell Temperature

$mC_{p\_module}$: Thermal capacity of the PV module

t: time

$Q_{in}$: Energy received due to solar irradiation, Equation 4.

$Q_{conv}$: Energy loss due to Convection

$Q_{elect}$: Electrical power generated

Interested readers in the detailed calculations of the terms; Qin, Qconv, and Qelect in Equation 4 are advised to consult references (Pei *et al.*, 2011; Sami and Marin, 2017; Sami, 2018) and Sami and Marin (2018).

### *2.3. Thermal Energy Incident in a PV Cell*

The thermal energy transferred from the PV cells to the Heat Transfer Fluid (HTF) is determined from the heat balance across the PV cell and HTF in terms of the heat transfer mechanisms; conduction, convection and radiation as follows (Faragali *et al.*, 2008; Sami, 2018; Sami and Campoverde, 2018).

$$Q_{conduction} = Q_{convection} - Q_{radiation} \quad (5)$$

The module back-surface temperature can be determined from the following;

$$Q_{conduction} = \frac{K_{Pv} \times \Delta T(T_c - T_m)}{L_{cell}} \quad (6)$$

$T_m$: Module Back-surface temperature

$K_{Pv}$: Thermal conductivity of PV cell

$L_{cell}$: Length of a PV cell

In addition, the heat transport fluid temperature is obtained after;

$$Q_{convection} = h_{water} \times \Delta T(T_m - T_f) \quad (7)$$

$Q_{convection}$: Energy due to convection

$h_{water}$: Heat transfer coefficient

$T_f$:Fluid temperature

To determine the heat transfer fluid flow rate and its temperatures at each element the finite-difference formulation is used. Each heat transfer fluid tube is divided into number of finite control volumes, and where thermophysical and thermodynamic properties are assumed constant at each element;

$$T_f = T_{f\_in} + \frac{\partial Q}{m_{water} C_p} \times t \quad (8)$$

$\dot{m}_w$: Water mass flow (HTF)

$C_p$: Specific heat of water.

t: time

δQ: the heat transfer per element

$T_{f\_in}$: Fluid temperature at inlet

The thermal energy transferred from the back of the PV cell to the heat transfer fluid (HTF) is obtained by;

$$Q_{Thermal} = \dot{m} \times C_{p\_water} \times \Delta T(T_{fHx+1} - T_{f\_In}) \quad (9)$$

Where;

$Q_{Thermal}$ : Energy from thermal process

$T_{fHx+1}$: Fluid temperature at thermal element (f+1)

$T_{f\_in}$: Fluid temperature at thermal element (1)

The total energy transferred to heat transfer fluid is calculated from the integration of Equations 6 through Equation 9 written for each element, dx, along the length of each tube. Interested readers in the integration process can be consult references (Faragali *et al.*, 2008; Liang *et al.*, 2015; Sami and Campoverde, 2018).

### *2.4. Nanofluid Heat Transfer Fluid*

Different investigators; Sharma *et al.* (2017) and Azo Material (2004) developed and reported on equations to calculate the specific heat, thermal conductivity, viscosity and density employing the law of mixtures. The data has shown that those equations were valid when compared with the experimental data.

The thermophysical, thermodynamic and heat transfer properties of nanofluids are determined in terms of the volumetric concentration of the nano particles as per Equation 10;

$$\alpha_{total} = \alpha_{particles} + \alpha_{base\ fluid} \quad (10)$$

Where α represents thermophysical property of the nanofluid.

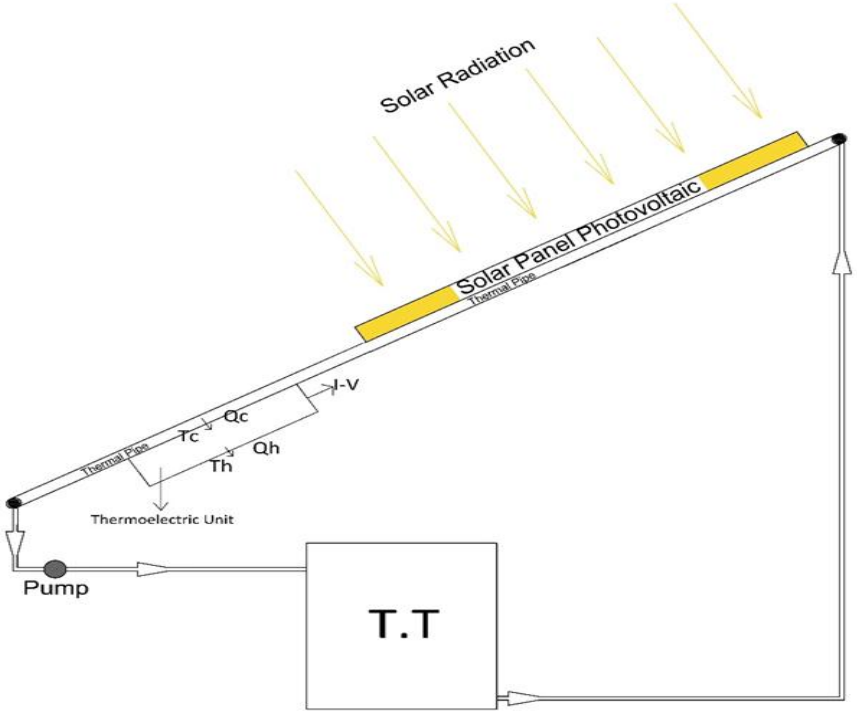


**Figure-1.** Integrated thermoelectric PV/Thermal hybrid system with Nanofluids.

The nanofluid thermal and thermophysical properties, $\alpha_{total}$ , can be calcualted as follows in Equation 11;

$$\alpha_{total} = \alpha_{base\ fluid} + \alpha_{particles}.(\Phi) \quad (11)$$

Where; Φ represents the nano particles volumetric concentration.

The thermal conductivity to thermal diffusivity and density of the nanofluids are related as Sami (2018); Sharma *et al.* (2017) as in Equation 12;

$$\lambda = \alpha\ \delta\ C_p \quad (12)$$

Where Cp is the specific heat, α is the thermal diffusivity, ʎ and ρ represent the thermal conductivity and density, respectively.

The specific heat is calculated for nanofluids as follows (Sharma *et al.*, 2017) as per Equation 13;

$$c_{pnf} = \frac{(1-\emptyset)(\rho Cp)_{bf} + \emptyset(\rho Cp)_p}{(1-\emptyset)\rho_{bf} + \emptyset\rho_p} \quad (13)$$

Where "nf" and "bf" refer to nanofluid and basic fluid, respectively. Ø is the nanofluid particle concentration. ρ represents the density.

The density of nanofluids can be written as follows (Sharma *et al.*, 2017), Equation 14;

$$\rho_{nf} = \emptyset_p\rho_p + (1-\emptyset)\rho_{bf} \quad (14)$$

### *2.5. Thermoelectric Model*

A voltage can be developed and detected at the terminals of a thermoelectric generator device as shown in Figure 2 when a temperature differential is maintained across the thermoelectric device. The voltage, called the Seebeck emf, is proportional to the magnitude of the temperature difference.

The heat balance across the thermoelectric unit shown in Figure 2 can be given by;

$$Q_c = Q_h + P_{out} \quad (15)$$

Where

$Q_c$ is thermal heat defined by Equation 9. $Q_h$ and $P_{out}$ represent the heat released to ambient and power output generated by the thermoelectric unit, respectively (Jatin *et al.*, 2016);

The thermal energy released $Q_h$ from the thermoelectric unit can be obtained by MATLAB iteration using the following equation and the energy balance in Equation 15, (Jatin *et al.*, 2016);

$$Q_h=(S_M \times Tc \times I)-(0.5 \times I^2 \times R_M)-(K_M \times DT) \quad (16)$$

Where;

$$S_M = s1 + s2T + s3T2 + s4\ T3 \quad (17)$$

And:

$S_M$ is the Seebeck coefficient of the module in volts/°K

T is the average module temperature in °K

Coefficients for a 71-cpl, 6-amp module are;

s1 = 1.33450 × 10-2

s2 = -5.37574 × 10-5

s3 = 7.42731 × 10-7

s4 = -1.27141 × 10-9

And;

$$S_M = (S_{MTh} - S_{MTc}) / DT$$

Where:

$S_{MTh}$ is the module's Seebeck coefficient at the hot side temperature Th

$S_{MTc}$ is the module's Seebeck coefficient at the cold side temperature Tc

$$R_M = r1 + r2\ T + r3T2 + r4T3 \quad (18)$$

Where:

$R_M$ is the module's resistance in ohms

T is the average module temperature in °K

Coefficients for a 71-cpl, 6-amp module are;

r1 = 2.08317

r2 = -1.98763 × 10-2

r3 = 8.53832 × 10-5

r4 = -9.03143 × 10-8

And;

$$R_M = (R_{MTh} - R_{MTc})/ DT$$

**Where:**

$R_M$ is the module's resistance in ohms

$R_{MTh}$ is the module's resistance at the hot side temperature Th

$R_{MTc}$ is the module's resistance at the cold side temperature Tc

$$K_M=k1+k2T+k3T2+k4T3 \quad (19)$$

Where,

$K_M$ is the module's thermal conductance in watts/°K

T is the average module temperature in °K

coefficients for a 71-cpl, 6-amp module are,

k1 = 4.76218 × 10-1

k2 = -3.89821 × 10-6

k3 = -8.64864 × 10-6

k4 = 2.20869 × 10-8

And;

$$K_M = (K_{MTh} - K_{MTc})/DT$$

**Where:**

K is the module's thermal conductance in watts/°K

$K_{MTh}$ is the thermal conductance at the hot side temperature Th

$K_{MTc}$ is the thermal conductance at the cold side temperature Tc

Finally, the temperature difference (DT) across the module in °K or °C is:

DT = Th - Tc

The output voltage ($V_{out}$) to the module in volts is:

$$V_{out}t=(S_M \times DT) + (I \times R_M) \quad (20)$$

The electrical output power ($P_{out}$) to the module in watts is:

$$P_{out}=V_{out} \times I \quad (21)$$

I – the output current to the module expressed in amperes

$V_{out}$ – the output voltage to the module expressed in volts

Th – the hot side temperature of the module expressed in °K

Tc – the cold side temperature of the module expressed in °K

The efficiency of the solar PV panels can be expressed as follows;

$$\eta_{pv} = \frac{Q_{elec}}{Q_{colector}} \quad (22)$$

Where, $Q_{elec}$ is calcualted by Equation 2 and, $Q_{colector}$ is obtained by Equation 3.

The thermal efficiency of thermal energy transferred to the heat transfer fluid HTF is;

$$\eta_{Qth} = \frac{Q_{th}}{Q_{colector}} \quad (23)$$

Where $Q_{th}$ is calcualted by Equation 9.

Finally, the hybrid system energy conversion efficiency for harnessing energy from solar energy using of integrated thermoelectric photovoltaic-thermal solar panel and nanofluids can be formulated as;

$$\eta_{sh} = \frac{Q_{th} + Q_{elec}}{Q_{colector}} \quad (24)$$

Where, $Q_{elec}$ is calcualted by Equation 2 and Equation 21. $Q_{th}$ is calcualted by Equation 9.

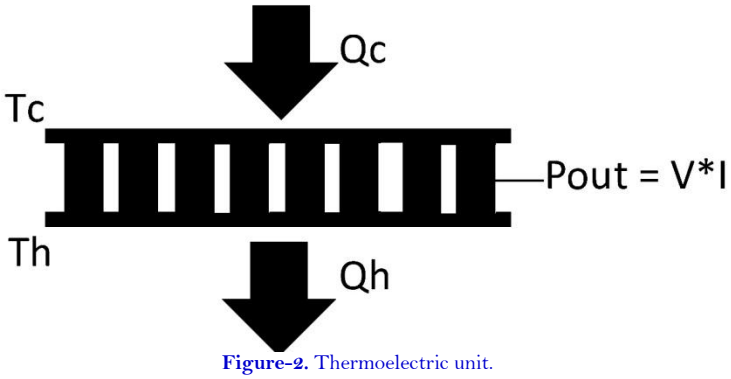


**Figure-2.** Thermoelectric unit.

## 3. NUMERICAL PROCEDURE

The model describing energy conversion process in the PV-Th panels, thermoelectric generator unit concept with nanofluids has been presented in Equation 1 through Equation 24. The flow diagram in Figure 3, was used solve the aforementioned equations. The calculation starts with the input of the parameters of the PV-Thermal solar panel, thermal tubes, thermoelectric generator device, nano particles; AI2O3, CuO, Fe304 and SiO2 and heat transfer fluid. The equations were integrated in the finite-difference formulations. Iterations were performed using MATLAB iteration techniques until a converged solution is reached. With the solar radiation the mass flow rate of the nanofluid circulating in the thin tubes welded to the PV solar collector is determined. Then the thermophysical properties and the heat transfer characteristics of the base fluid, water, and nanofluids at different concentrations are determined. This was accomplished by solving the finite-difference formulation of the aforementioned equations. Then the parameters describing the behavior of PV-Thermal solar panels, thermoelectric generator unit were determined. Finally, the individual and hybrid system efficiencies were calcualted.

## 4. DISCUSION AND ANALYSIS

Equation 1 through Equation 24 have been coded in finite-difference forms, integrated and numerically solved as per the logical diagram in Figure 3. Samples of the predicted results for the PV-Thermal solar panel and thermoelectric generator, including the thermal heat dissipated by the PV solar panel and absorbed by heat transfer fluid HTF with various nano particles; AI2O3, CuO, Fe304 and CiO2 that drives the thermoelectric unit are presented at different inlet conditions hereby. In the following sections, we also present the analysis and discussions of these numerical results as well as the validations of the proposed simulation model at temperature difference of 15 °C across the thermal tube. It is worthwhile noting that the numerical simulation presented was performed under different conditions such as; PV cell temperatures from 10°C through 70°C, ambient temperatures from 10°C through 38°C and solar radiations; 550, 750, 1000 and 1200 w/m$^2$.

The PV collector's specifications in this study are obtained from Faragali *et al.* (2008). The characteristic curves of the PV solar panel are also obtained from the manufacturer's specification sheet (Faragali *et al.*, 2008). Interested readers in the full disclosure of the PV parameters are advised to consult (Faragali *et al.*, 2008).

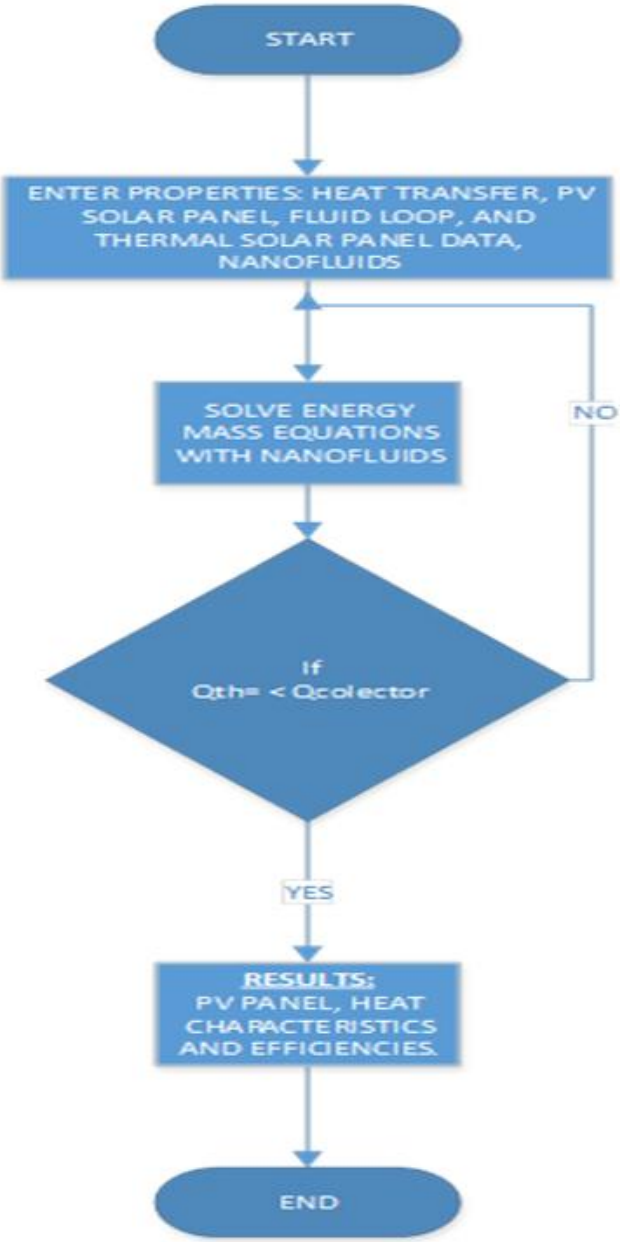


**Figure-3.** Logical flow diagram for finite difference scheme.

It is also assumed in this simulation that the PV cells are commercial grade monocrystalline silicon cells with electrical efficiency of 12%, and have a thermal coefficient, of 0.54% [1/K] (Faragali *et al.*, 2008). The cooling thin thermal tubes/heat exchanger pipes are bonded to the back of the PV solar model without any air gap to ensure complete heat transfer by conduction, convection and radiation to the nanofluid in the thermal tubes.

The values of SM, RM, and KM are calcualted expressed by Equations 16 through Equations 21. These coefficients used over a range of -100°C to +150°C, were according to the industry-standard thermoelectric unit 71-couple, 6-ampere module; TEC1-127-06L. Interested readers in the specifications of this module are advised to consult references (Jatin *et al.*, 2016). It should also be noted that the ambient temperature is considered as 25 °C for the thermoelectric calculations. The thermoelectric generator device was attached appropriately to the heat sink, so that heat capacity or dissipation at bottom side surface of the module was maximized.

As discussed, in order to solve Equation 1 through Equation 24 the thermal and thermophysical properties of the nanofluids; AI2O3, CuO, Fe304 and SiO2 were obtained from references (Choi, 1995; Azo Material, 2004; Kakaç and Pramuanjaroenkij, 2009; Taylor *et al.*, 2011; Bachock and Pop, 2012; Saleh, 2012; Khullar *et al.*, 2013; Chaudhari

and Walke, 2014; Nerella *et al.*, 2014; Allen, 2015; Kasaeian *et al.*, 2015; Sagadevan, 2015; Sharma *et al.*, 2017; Sami, 2018; Sami, 2018). Allen (2015) studied the impact of magnetic field on the thermal conductivity of nanofluids and obtained the thermal conductivity for each nanofluids such as AI2O3, CuO, Fe304 and SIO2 at different magnetic fields. His data at zero magnetic field among the other references were considered in this study.

In the following, analysis of the results are presented for thermal heat dissipated by the PV solar panel, behavior of thee PV-Th, and thermoelectric generator device as well as system efficiencies under nanofluid flows from 0,00697 kg/s to 0.0345 kg/s, nano particles volumetric concentrations from 0.01 to 0.5 and under solar radiations from 550 W/m² to 1200 W/m². It should also be noted that the design of the thermal tubes welded to the back of the PV solar panel was based upon mass flow rate of 0.00697 kg/s at 550 W/m² solar radiation.

Average solar irradiations were used in the simulation of the Photovoltaic collectors. The recording of the ambient conditions showed that the relative humidity is stable during the various hours of the day. Therefore, the relative humilities were assumed constant.

The dynamic behavior of the PV cell, PV back temperatures have been presented in Figure 4 and Figure 5, at different solar radiations with water as the base fluid. Furthermore, the aforementioned figures together with Equations 3 through Equation 9, demonstrate clearly that an increasing the PV cell temperature increases in the back-cell temperature and consequently the fluid temperature due to the heat transfer from solar energy by conduction and convection as well as radiation, respectively. In additions, these figures and Equations 3 through 9 also show that the higher the solar radiation the higher the PV cell temperature, and the PV back temperature. And also, these figures show that the cell temperature reaches its maximum design temperature after 1200 seconds depending upon the solar radiation (Sami and Campoverde, 2018).

The Figures 4 and Figure 5 also show provide that the higher PV cell temperature increases the back cell and the fluid temperatures (Sami and Campoverde, 2018). It is quite evident from the results presented in these figures that the cell temperatures increase with the increase of solar radiation. This can be shown by these figures and Equations 3 through 9. This has been reported and discussed in the literature where similar observations were presented in references namely, Sami and Campoverde (2018); Sami (2018); Sami and Marin (2017); Sami and Rivera (2017); Sami and Marin (2017); Good *et al.* (2015); Faragali *et al.* (2008).

To evaluate the performance of the PV-Th and TEG hybrid module, current-voltage characteristics of the TEG device were separately investigated under several operating conditions. An important parameter to optimize the PV and TEG hybrid module efficiency is the power output at TEG device. Current-voltage curves and other characteristics of the TEG hybrid under solar radiation of 750 w/m² and different concentrations of the nanofluid AI2O3 were presented in Figures 6 through Figure 9.

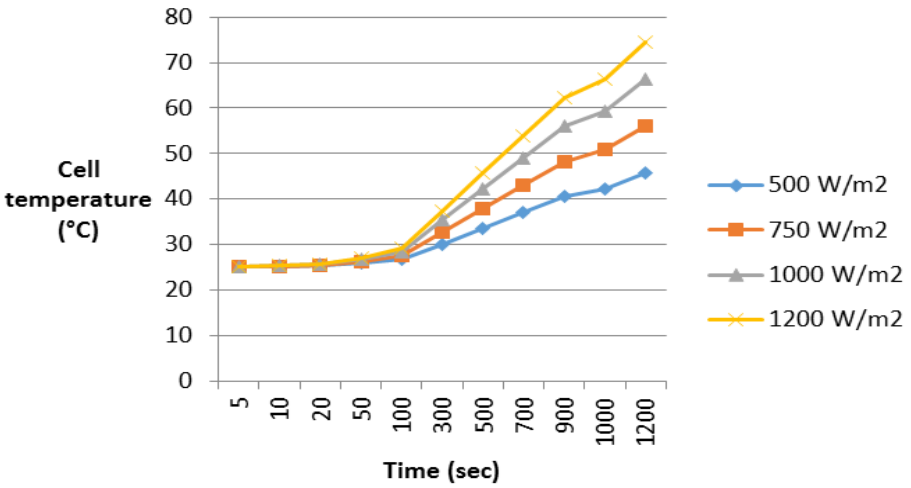


**Figure-4.** PV Cell temperature at different solar radiations and temperature difference 15 °C (Sami and Campoverde, 2018).

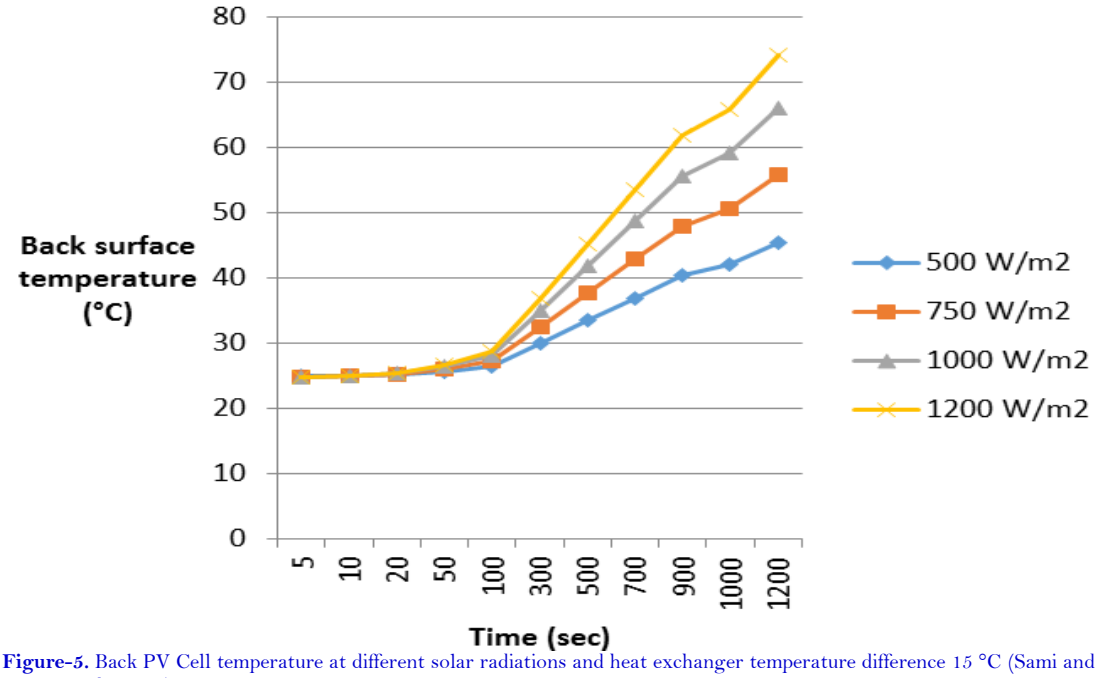


**Figure-5.** Back PV Cell temperature at different solar radiations and heat exchanger temperature difference 15 °C (Sami and Campoverde, 2018).

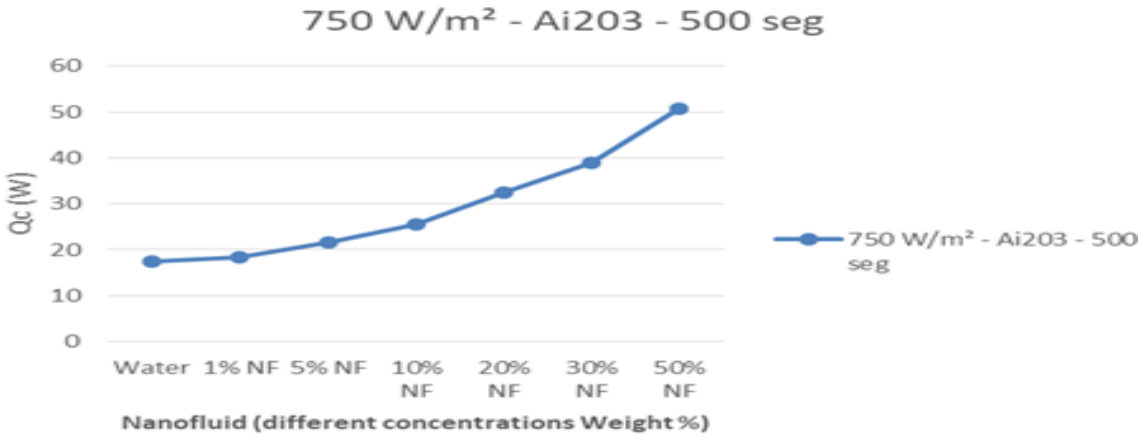


**Figure-6.** Thermal energy dissipated to the heat transport fluid at different concentrations of Nanofluid AI2O3 and 750 w/m2.

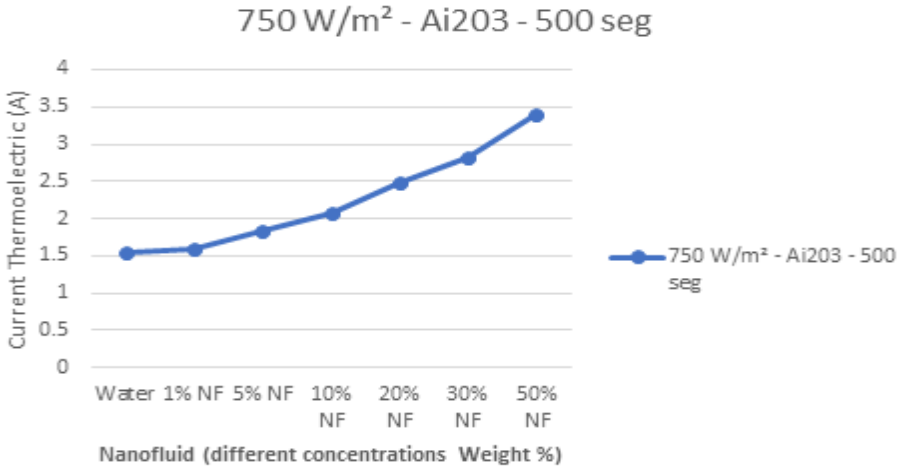


**Figure-7.** Current thermoelectric at different concentrations of Nanofluid AI2O3 and 750 w/m².

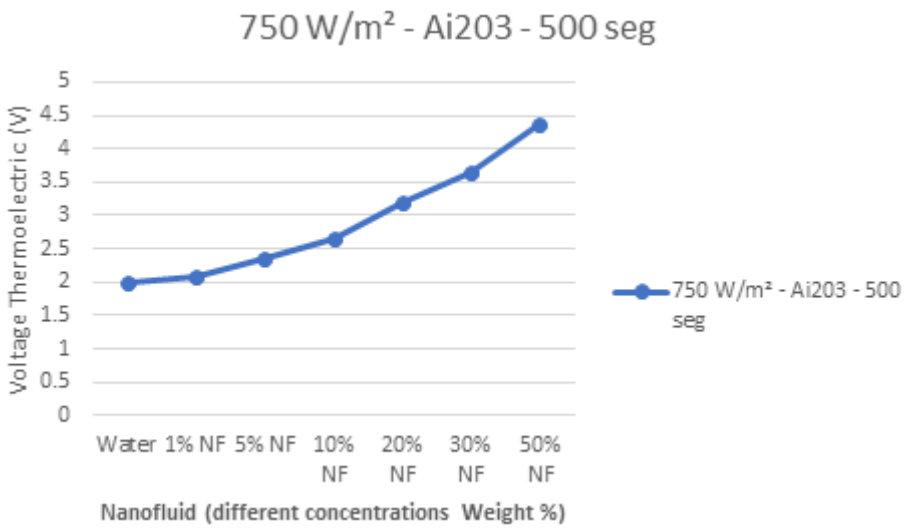


**Figure-8.** Voltage thermometric at different concentrations of Nanofluid AI2O3 at 750 w/m².

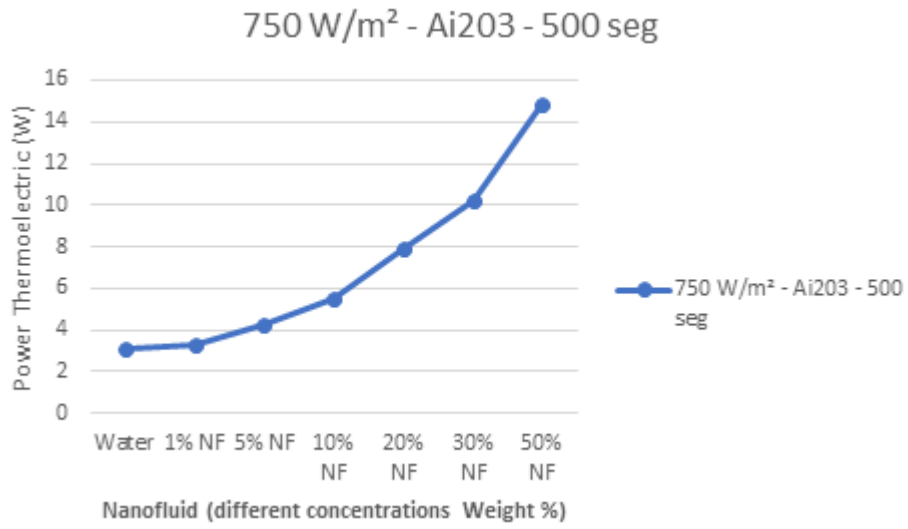


**Figure-9.** Power thermoelectric at different concentrations of Nanofluid AI2O3 at 750 w/m².

The data displayed in Figure 6 shows that the nanofluids significantly contributed to the enhancement of the key critical parameter of the PV-Thermal hybrid system in question; thermal energy dissipated from the PV-Th panel over that of the water flow as base fluid. It can be also noted from this figure that higher nanofluid concentration enhances the thermal energy absorbed by the heat transfer fluid.

Figures 7 through Figure 9 display the Current-voltage curves of the thermoelectric generator module under different nanofluids volumetric concentrations. It can be seen from these figures that the higher the nanofluids concentrations the higher the current-voltage and power output.

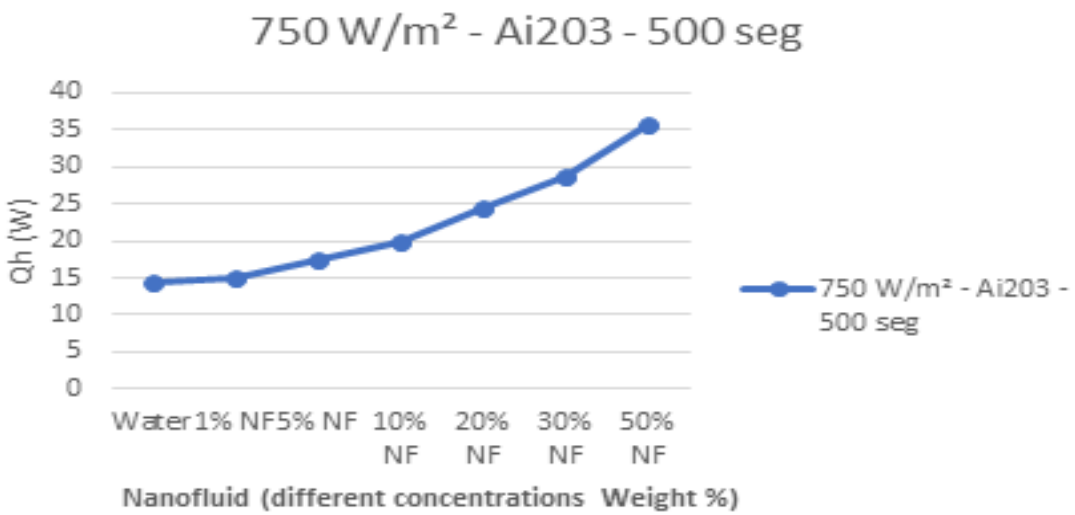


**Figure-10.** Thermal energy dissipated from thermoelectric at different concentrations of Nanofluid AI2O3 at 750 w/m².

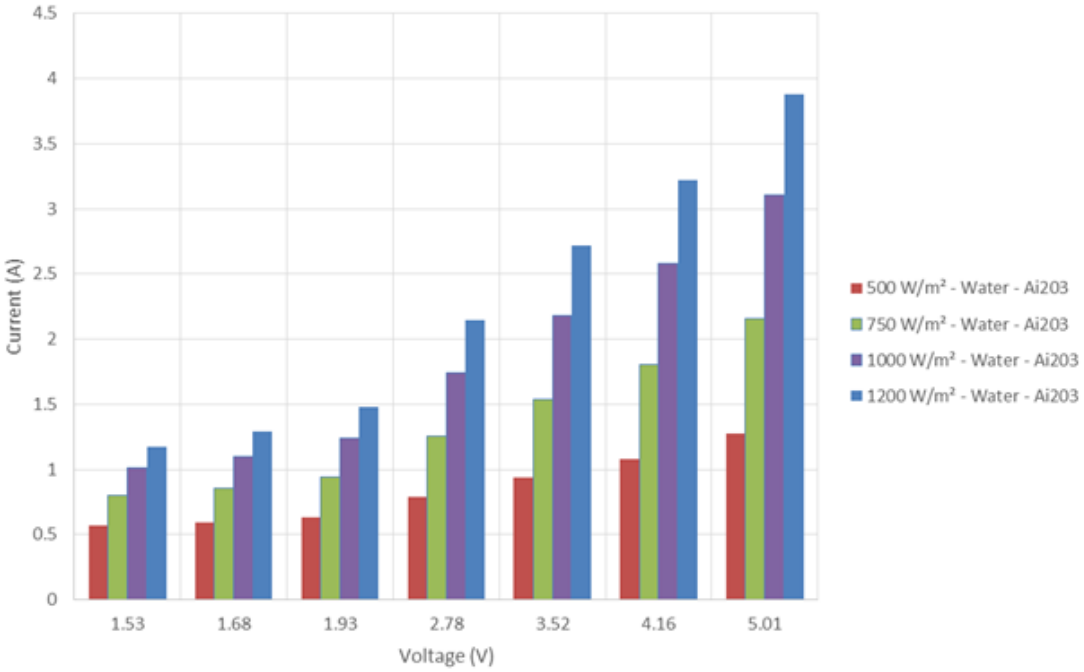


**Figure-11.** Thermoelectric V-A characteristics for water at 500 seconds and different concentrations of solar radiations.

The impact of the nanofluid AIO203 concentrations on the thermal heat released from the thermoelectric generator module to the sink temperature, ambient condition is demonstrated in Figure 10. Where the simulated results clearly show that higher the nanofluid's concentration increases the thermal heat transferred over that of the water as base fluid. This figure together with Figure 6 also demonstrate the benefits of using nanofluids in enhancing the thermal heat recovered from the PV-Th collectors and released to the ambient, respectively. This enhancement of the critical parameters of the PV-Thermal and thermoelectric generator in the hybrid system with other nanofluids other than AIO203 will be discussed elsewhere in the paper.

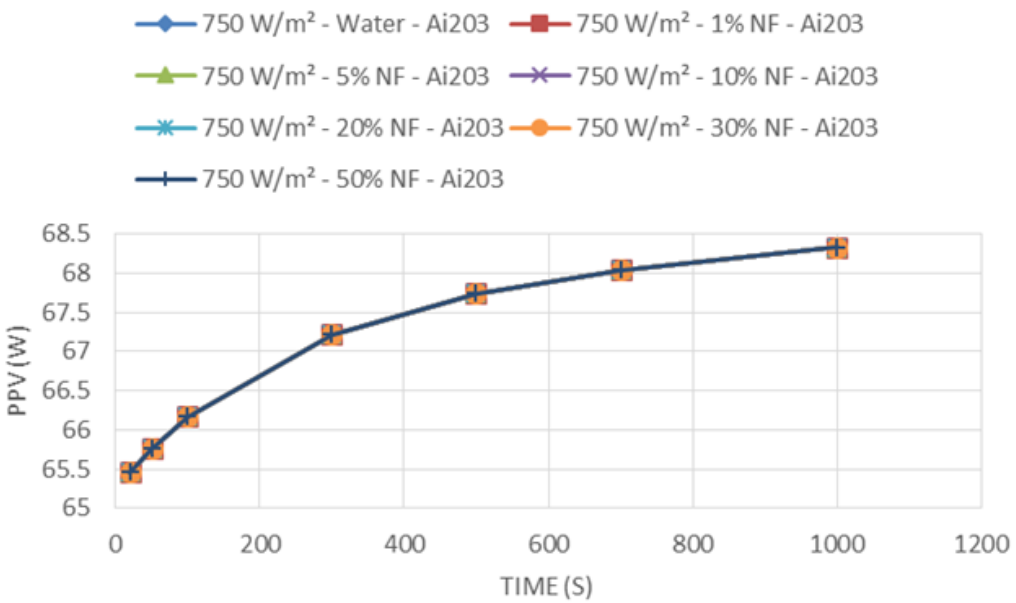


**Figure-12.** PV solar panel output at different concentrations of Nanofluid AiO2 at 750 w/m².

On the other hand, the numerical results shown in Figure 12 show that the solar PV panel output at different concentrations of Nanofluid AIO2 at 750 w/m2. It can be noticed also from this figure that the solar PV output is independent of the concentration of the nanofluids and depends only on the solar PV collector's characteristics and solar radiations at the site as reported in the literature namely references (Chaudhari and Walke, 2014; Kasaeian *et al.*, 2015; Sagadevan, 2015; Sami, 2018; Sami and Campoverde, 2018).

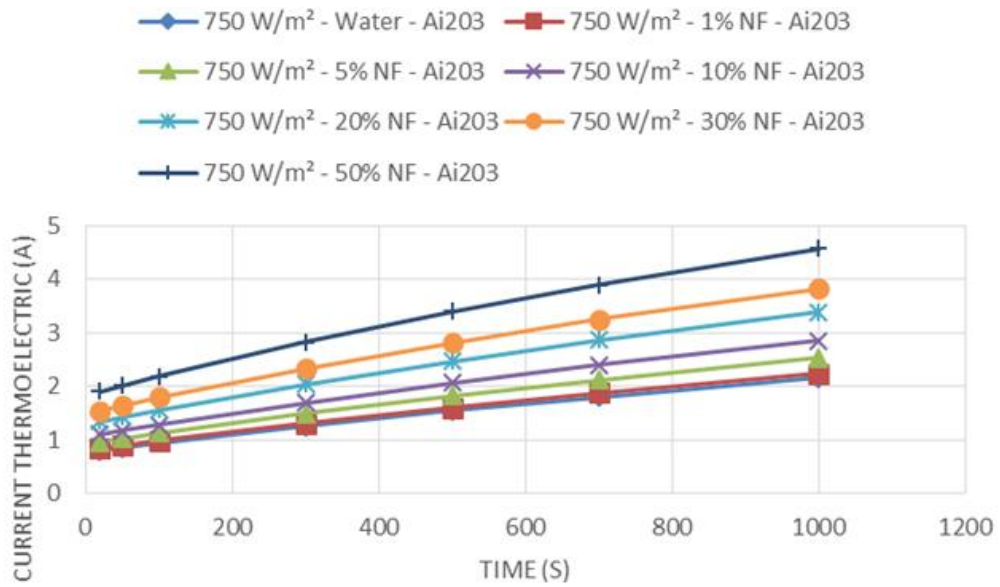


**Figure-13.** Thermoelectric current at different Time and concentrations of Nanofluid AIO2 at 750 w/m².

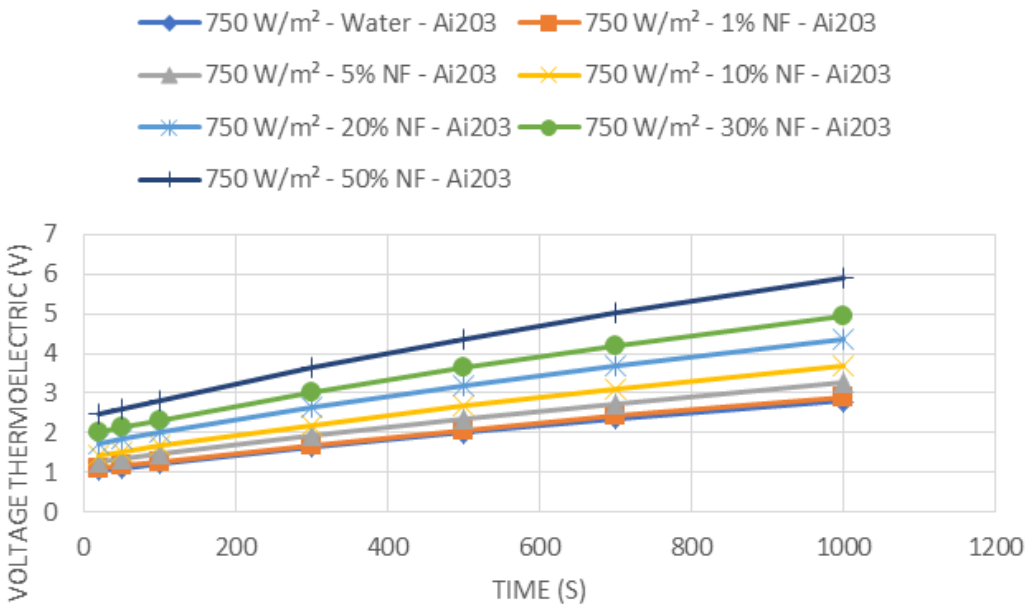


**Figure-14.** Thermoelectric voltage at different Time and concentrations of Nanofluid AIO2 at 750 w/m².

The impact of the nanofluid AIO203 concentrations on the behavior of the PV-Th and thermoelectric hybrid system is presented in Figures 13 through Figure 18. It can be observed from these figures that the higher the nanofluid concentration the better the performance of the hybrid system in question. In particular Figures 13 and Figure 14 showed the impact of the nanofluid AIO203 on the power output of the thermoelectric generator device, where the higher the nanofluid concentrations the higher the output current, voltage as well as power over that of the water as base heat transfer fluid. It is quite evident that 50%, AIO203 nanofluid concentration produces the higher power output characteristics, however, it's extremely important to examine and take into account the pressure drop and other side effects associated with higher concentrations on the flow conditions and system efficiency. These figures also demonstrate the benefits of using nanofluids in enhancing the thermal heat recovered from the PV-Th collectors that drives the thermoelectric generator device. The impact of other nanofluids other than AIO203 on the critical parameters of the PV-Thermal and thermoelectric generator device will be discussed elsewhere in the paper.

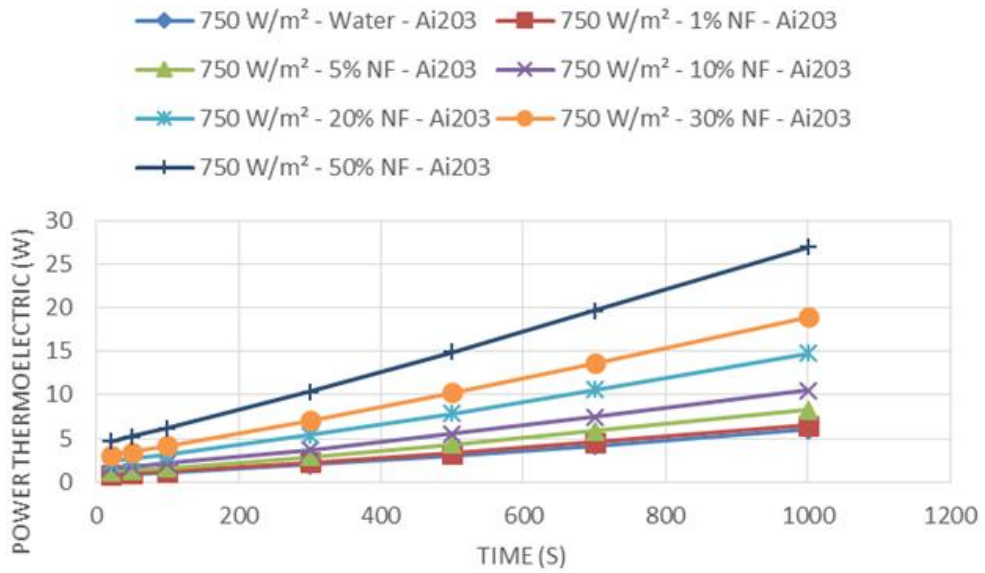


**Figure-15.** Thermoelectric power at different Time and concentrations of Nanofluid AIO2 at 750 w/m².

The thermal heats released by the PV-Th solar panel and the thermoelectric generator device are displayed in Figures 16 and 17, respectively. It can be seen that as the concentration of the nanofluid AI203 particles increase over the water as basic fluid, the heat released by the PV-Th and thermoelectric generator device increases. In our opinion, the higher nano particle concentrations increase the thermal, thermophysical and heat transfer properties of the nanofluid such as specific heat, density, thermal conductivity and viscosity as well as the convection heat transfer coefficient. This in turn enhances the thermal heat absorbed by the nanofluid.

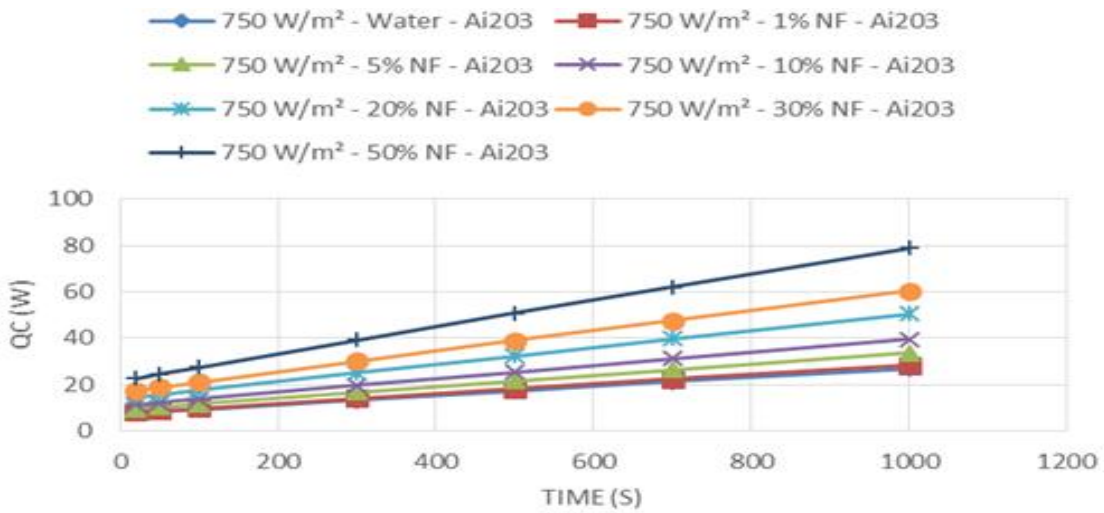


**Figure-16.** Thermoelectric heat released to ambient at different Time and concentrations of Nanofluid AIO2 at 750 w/m².

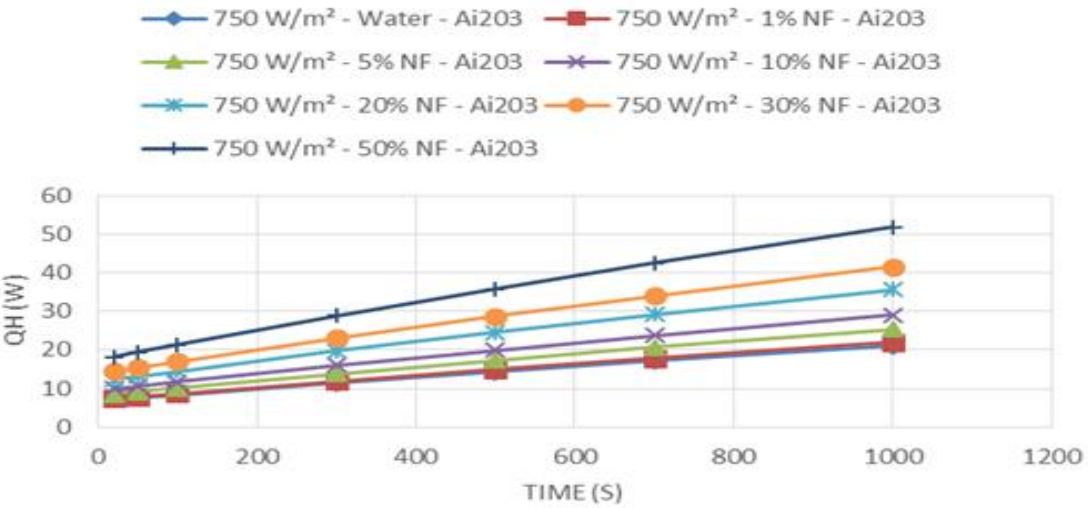


**Figure-17.** Thermoelectric heat released to ambient at different Time and concentrations of Nanofluid AIO2 at 750 w/m².

The thermoelectric generator device and the hybrid system efficiencies are presented in Figures 18 and 19, respectively. The results in these figures show that higher the AIO203 nanofluid's concentration enhance the efficiency of the thermoelectric device and the hybrid system over that of the water as base heat transfer fluid. The effect of other nanofluids other than AIO203 on the efficiencies of thermoelectric generator device and the hybrid system will be discussed elsewhere in the paper.

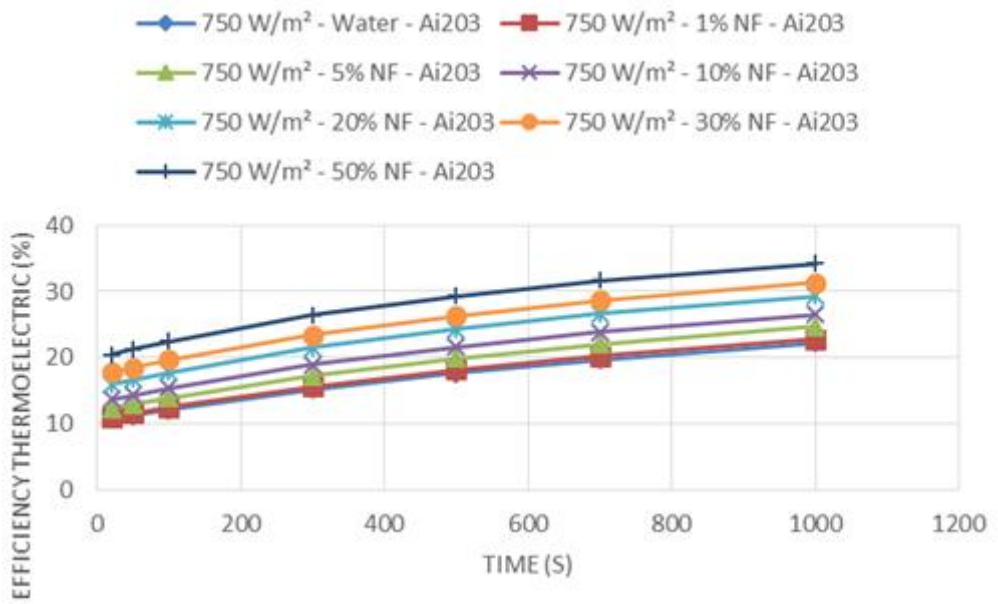


**Figure-18.** Thermoelectric efficiency at different concentrations of Nanofluid AI203 at 750 w/m².

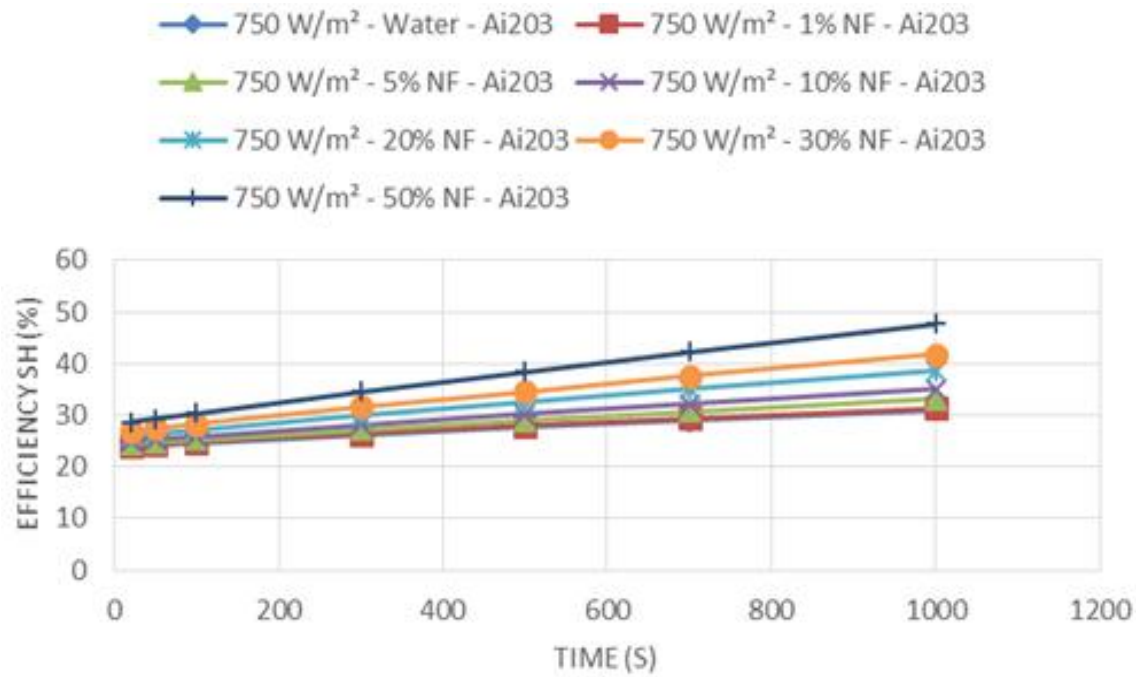


**Figure-19.** Efficiency of hybrid; solar PV-Th and thermoelectric at different concentrations of Nanofluid AIO203 at 750 w/m².

On the other hand, Figure 20 through Figure 25, demonstrates the effect of the solar radiation on behavior of PV-Th and thermoelectric generator device system using nanofluid AIO203. In general, the results displayed in these figures clearly show that the higher the solar radiation the higher the thermal heat released from the PV-Th solar panel to the heat transfer fluid, the higher the power produced by the thermoelectric device and also the higher the efficiencies. It is also obvious from these figures that the higher the nanofluid AIO203 concentrations the higher the aforementioned parameters of the hybrid system over the water as basic working fluid.

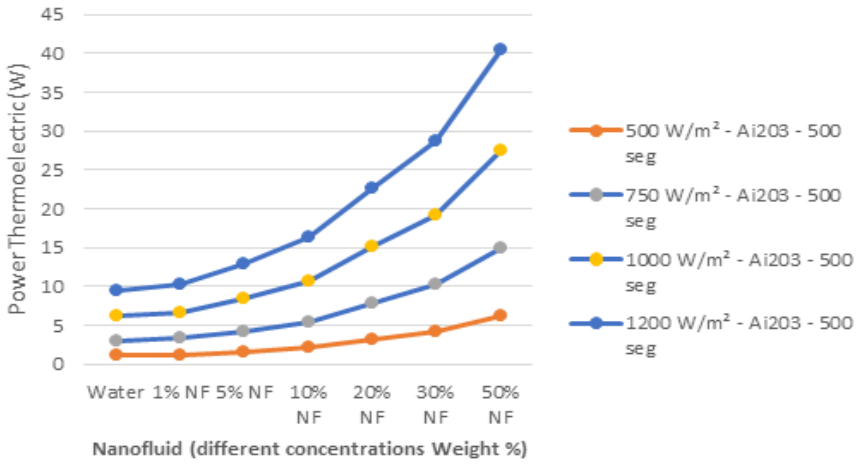


**Figure-20.** Thermoelectric power at different solar radiations.

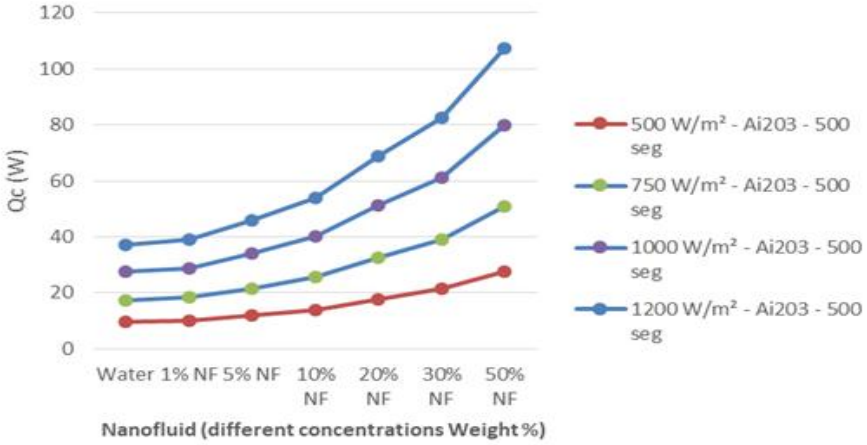


**Figure-21.** Thermal energy transferred to HTF at different solar radiations.

In particular Figure 20 shows the thermoelectric power generated due to the thermal energy C.F. Figure 21 applied at the thermoelectric device at different solar radiations using nanofluid AIO203. Those two figures indicate that higher solar radiations enhance the thermal heat transfer to the thermoelectric device and its power produced.

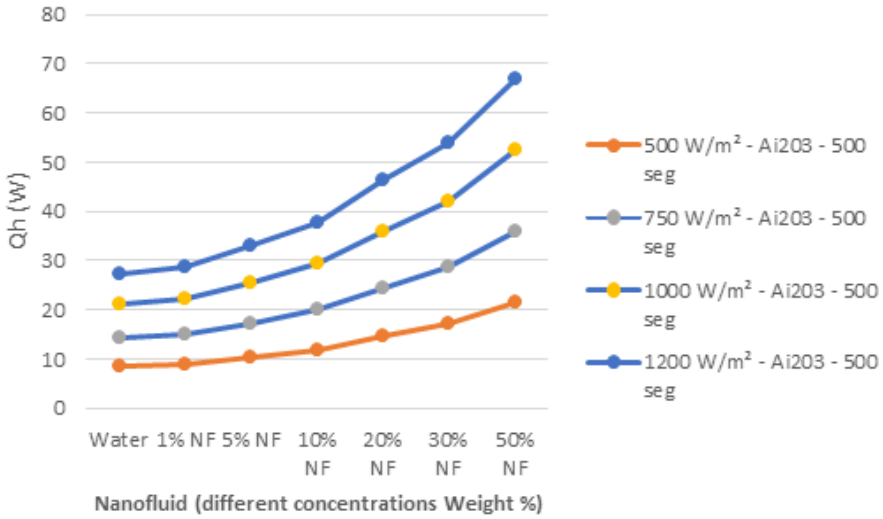


**Figure-22.** Thermal energy released from thermoelectric device at different solar radiations.

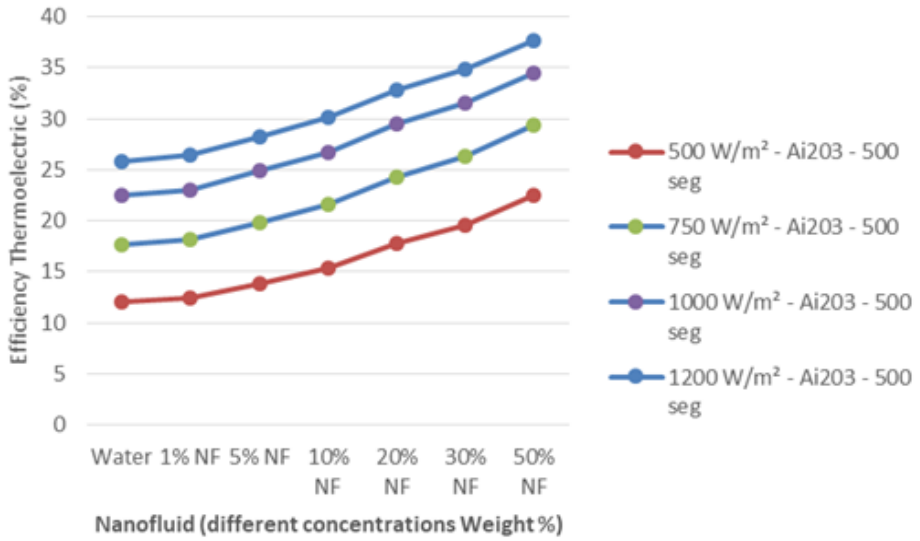


**Figure-23.** Thermoelectric efficiency at different solar radiations.

On the other hand, Figures 25 through 29 display the impact of using different nanofluids suspended particles of the AIO203, CuO, Fe304 and SIO2, on the thermoelectric generator characteristics including efficiencies of thermoelectric and hybrid system, respectively. In these figures the nanofluid concentration varies between 0.01 to 0.50 with solar radiation of 750 w/m² with the different parameters numerically calcualted at 1000 seconds. Also, the results in these figures show higher the concentration of nanofluid enhances the characteristics of the thermoelectric generator over water as basic fluid. In our opinion, these observations can explain that higher nano particle concentrations enhance heat transfer properties of the heat transfer fluid such as specific heat, density, thermal conductivity and viscosity as well as the convection heat transfer coefficient.

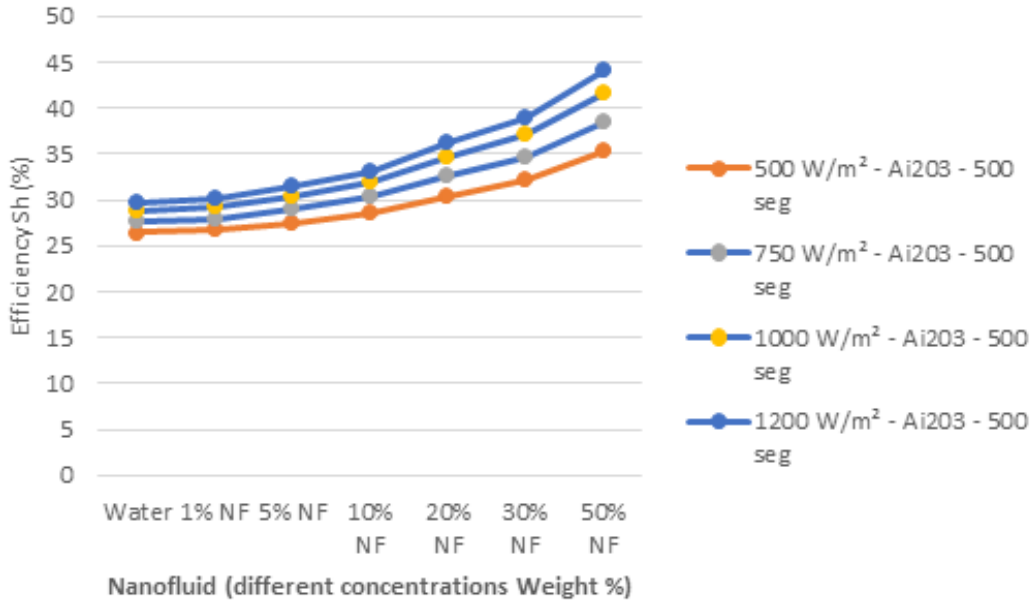


**Figure-24.** Hybrid system efficiency at different solar radiations.

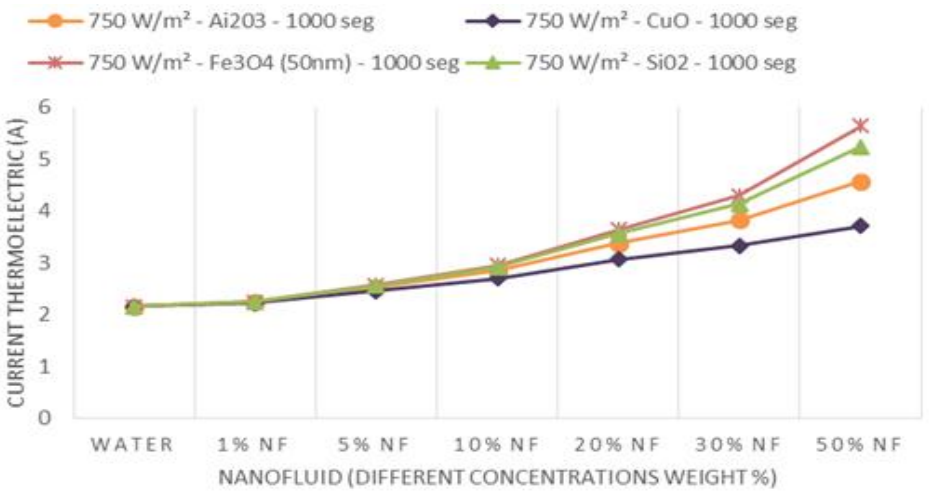


**Figure-25.** Thermoelectric current at different nanofluids.

That increases, stimulates and drives more heat transfer from the PV-Th solar panel into the nanofluid. This in turn also drives more heat into the thermoelectric generator device and generates more power and enhances its efficiencies. It is also worthwhile noting that the PV solar panel output power and PV solar panel efficiency remain constant and is fully not dependent of the nanofluids concentrations.

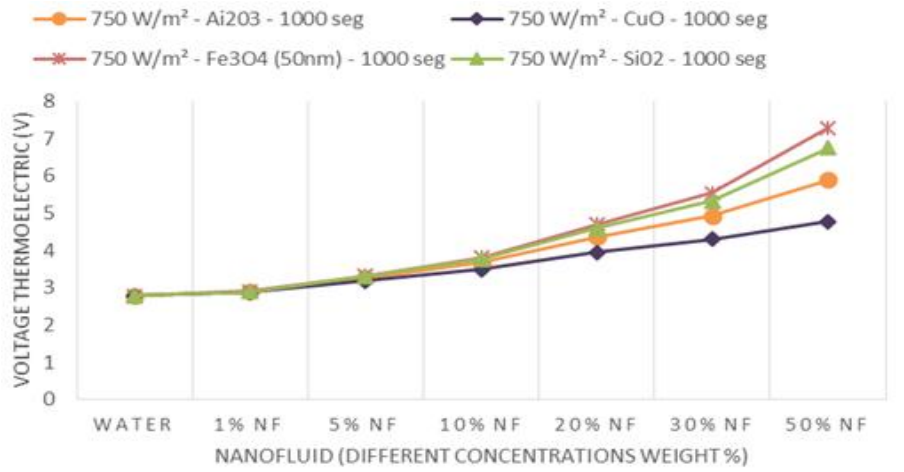


**Figure-26.** Thermoelectric voltage at different nanofluids.

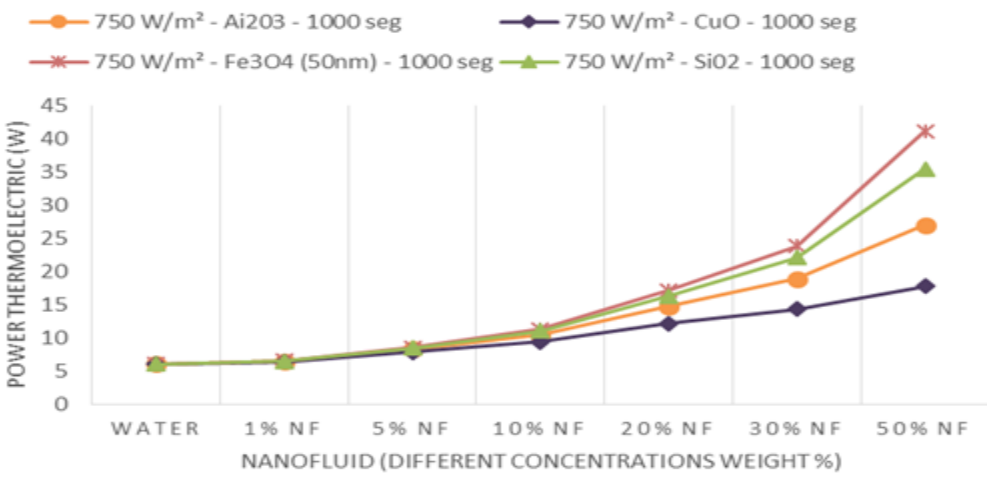


**Figure-27.** Thermoelectric output power at different nanofluids.

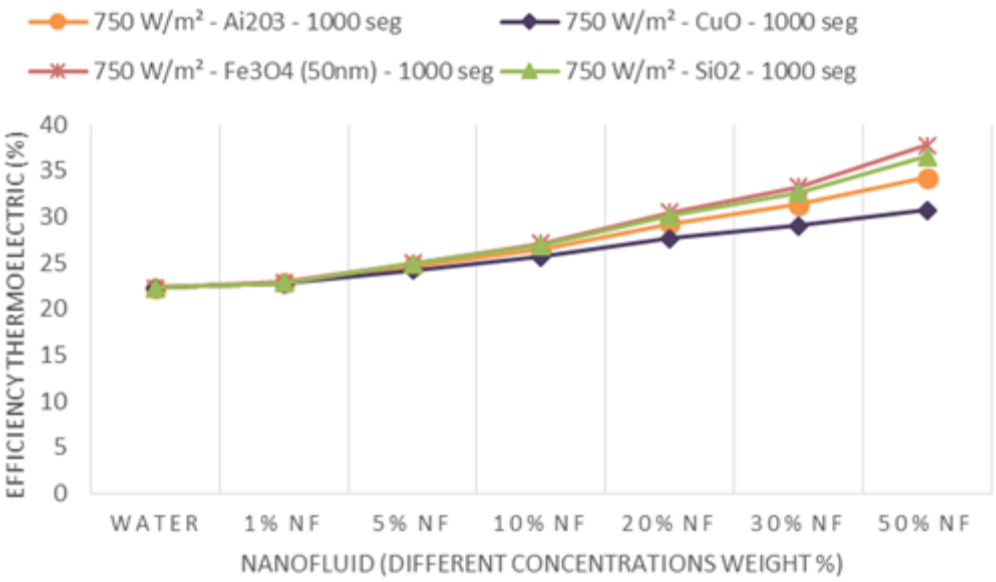


**Figure-28.** Thermoelectric efficiency at different nanofluids.

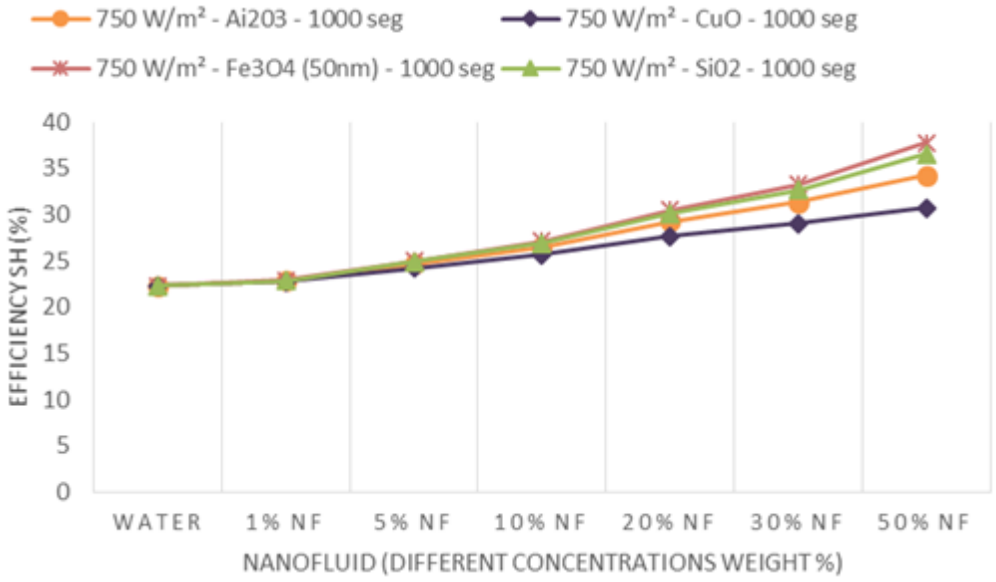


**Figure-29.** Hybrid system efficiency at different nanofluids.

Furthermore, the results displayed in Figures 25, through Figure 29 for solar radiation of 750 w/m² indicated that that the thermoelectric generator device characteristics were significantly higher with the use of nanofluid Fe304 and they increase as the concentration of this nanofluid particles increases over the water as basic heat transfer flow. It is also believed that this is attributed to the higher thermophysical and thermodynamic as well as heat transfer properties of nanofluid Fe304 compared to the other nanofluids under investigation. On the other hand, the numerical results displayed in Figures 27 through 29, gave clear evidence that the thermoelectric generator and hybrid efficiencies at 750 w/m2 solar radiations were enhanced by the use of nanofluid Fe304 over the basic fluid, water. In addition, Figures 30 and Figure 31 recorded at 1000 seconds, clearly demonstrate that at higher solar radiation, the nanofluid Fe304 enhance the thermoelectric generator and hybrid system efficiencies over the base fluid water.

Furthermore, at low nanofluid concentration of 1% there is no noticeable difference of the impact of the nano particles of the AI2O3, Fe304, CuO, and SiO2. However, at concentrations higher than 10%, it is quite evident that Fe304 and other nanofluids have the greatest impact on the thermoelectric generator device parameters.

Furthermore, the study reported by Maiga *et al.* (2005) on fully developed turbulent flow of Al2O3- water nanofluid flow in circular tube at uniform heat flux clearly confirms our findings that the inclusion of nano particles into the base fluids has produced a considerable augmentation of the heat transfer coefficient, thermal heat transferred. Clearly Figures 25 through 29 show that increases is dependent on the particle concentration. This is also in agreement with what has been reported in the literature namely; in references (Sami, 2018) through (Khullar *et al.*, 2013).

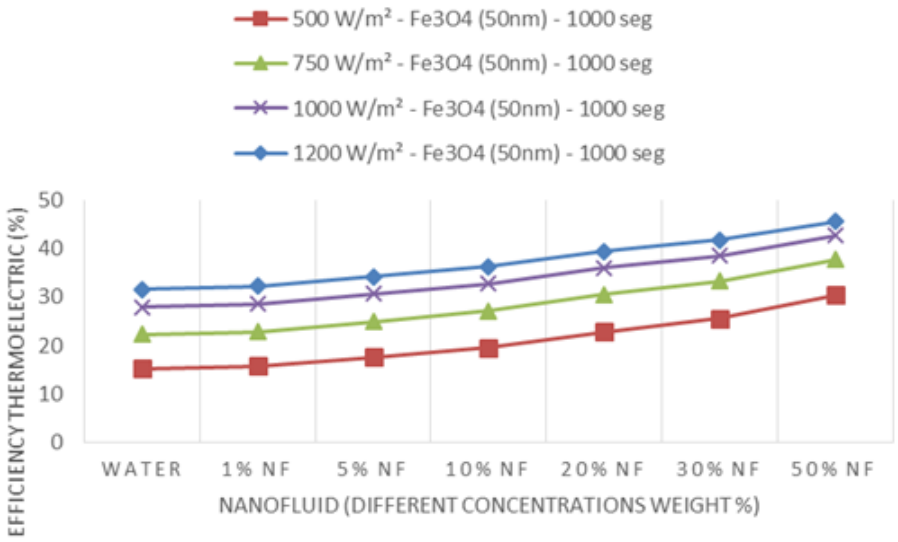


**Figure-30.** Thermoelectric device efficiency at different solar radiations.

As per Figure 32, it is can also observed during this study that higher the mass flow rate of the nanofluids increases the thermal energy absorbed by the heat transfer fluid. This finding is in agreement with what has been reported in the literature namely references (Choi, 1995; Kakaç and Pramuanjaroenkij, 2009; Taylor *et al.*, 2011; Bachock and Pop, 2012; Saleh, 2012; Khullar *et al.*, 2013; Chaudhari and Walke, 2014; Nerella *et al.*, 2014; Allen, 2015; Kasaeian *et al.*, 2015; Sagadevan, 2015; Sharma *et al.*, 2017; Sami, 2018; Sami, 2018). Consequently, the thermoelectric generator and hybrid efficiencies have the highest values at the higher heat transfer fluid flow. Therefore, it is quite significant and critical for the thermoelectric generator device presented in this research work to be designed at the optimum heat transfer flow as well as the optimum solar radiation in order to ensure higher thermoelectric generator power produced and also higher hybrid efficiency.

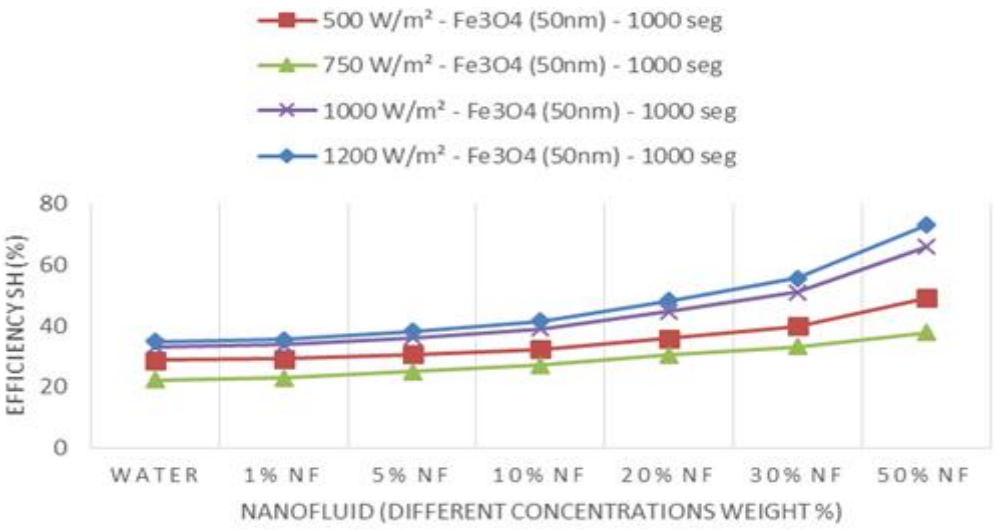


**Figure-31.** Hybrid system efficiency at different solar radiations.

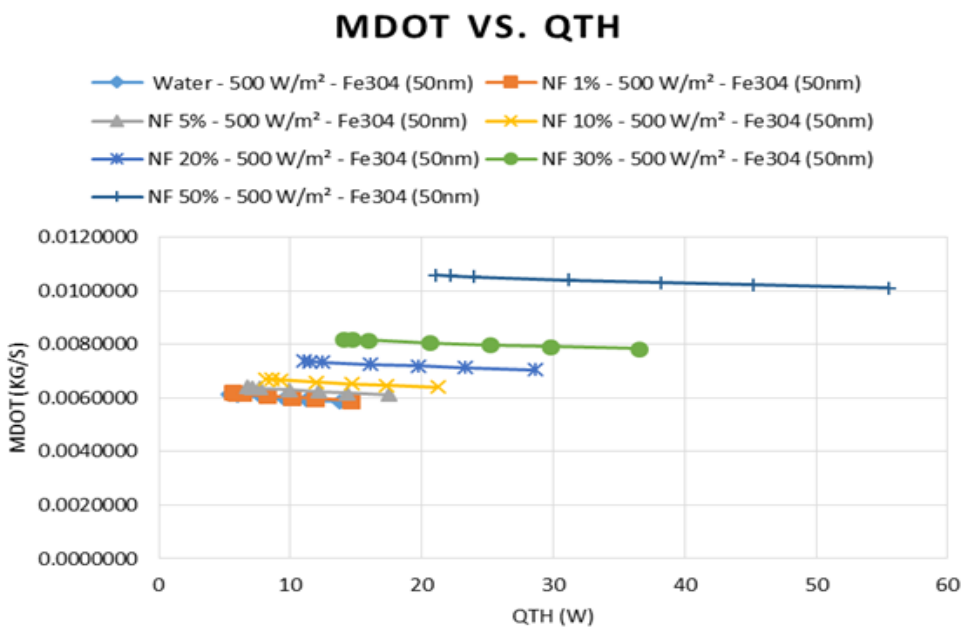


**Figure-32.** Heat transfer flow at different nanofluid concentrations.

Ones of the most frequent nanofluids studied in the literature are the Fe304 and AI2O3 see C.F. Figures 25 through 29. The results displayed in these figures and Figure 32 show that higher concentration of nanofluid Fe304, increases the mass flow rate of nanofluid and the thermal energy absorbed by the heat transfer fluid. Consequently, the thermoelectric generator device and hybrid system efficiency efficiencies have the highest values at the higher heat transfer fluid flow. This is quite significant and critical since this research work has been conducted to optimize the performance of the thermoelectric devices and PV-Th solar panel and the hybrid system efficiency.

### *4.1. Model Validation*

This section is intended to validate the model prediction of the different parameters the PV-Th and thermoelectric generator device presented in Equations 1 through Equation 24.

Figure 33 displays a comparison between the model prediction of the temperature of and data of Faragali *et al.* (2008). The data showed that the model fairly compares with the data reported by Faragali *et al.* (2008). This figure showed that the model and data have some discrepancies exit. It is believed that the discrepancies are due to the fact that the various parameters used in Equations 6 through 9 were not fully disclosed by Faragali *et al.* (2008). However, same observations were reported in references (Liang *et al.*, 2015; Sami, 2018; Sami and Campoverde, 2018).

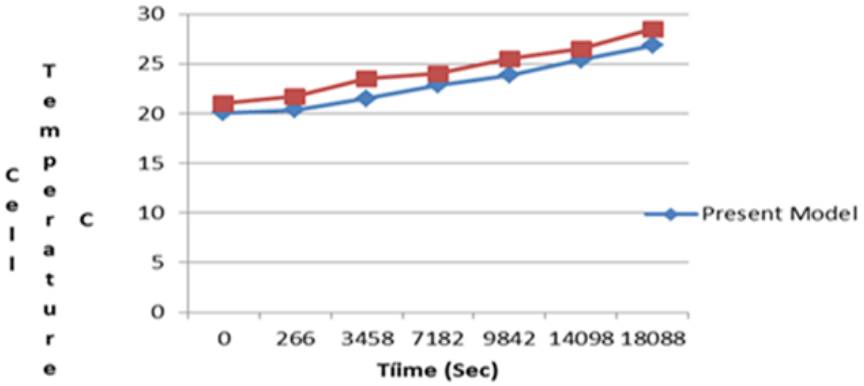


**Figure-33.** Comparison between model prediction and experimental data (Faragali *et al.*, 2008).

Thermoelectric generator experimental data is scared in the literature. Recently Data published by Al Musleh *et al.* (2017) on thermoelectric generator with very low-low temperature difference between the hot and cold sides were selected for validating our model. The experimental results reported in Al Musleh *et al.* (2017) used a thermoelectric generator TEG experimental test setup with temperature-controlled hotplate in order to provide accurate TEG performance. Data at the very-low-temperature difference were simulated and compared to our model numerical prediction and presented for power and heat in Figure 34 and Figure 35 respectively.

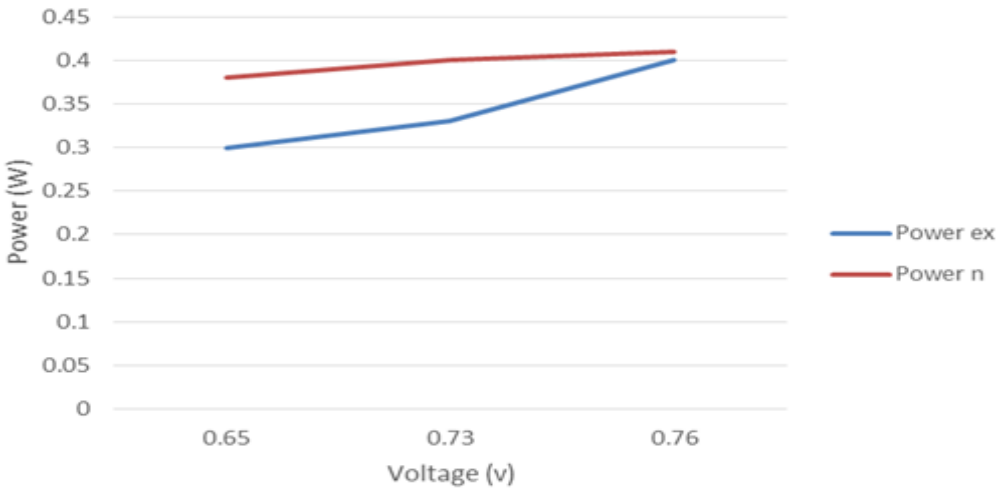


**Figure-34.** Comparison between model prediction of TEG power and experimental data (Al Musleh *et al.*, 2017).

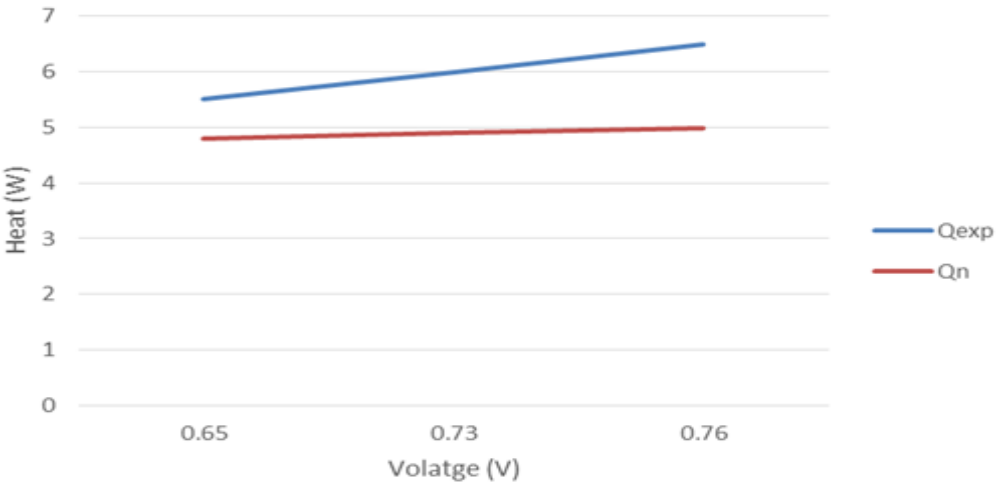


**Figure-35.** Comparison between model prediction of TEG heat and experimental data (Al Musleh *et al.*, 2017).

The temperatures of the driving heat source (hotplate) to the TEG were matched with the temperatures of the heat transport fluid heated by thermal energy dissipated from the PV-Th solar panel due to solar radiation. In general, as shown in Figure 34, our model's prediction compared fairly with the data reported by Al Musleh *et al.* (2017) of voltage across the TEG. Furthermore, Figure 35 demonstrated that our model also fairly predicted the TEG power data of reference (Al Musleh *et al.*, 2017). There are discrepancies observed in two figures, where our model underpredicted the power and over predicted the heat experimental data. In our opinion, the discrepancies between our model's prediction and the data of reference (Al Musleh *et al.*, 2017) are attributed to the fact our model does not take into consideration the heat losses from the TEG during the energy conversion process and also due to inaccuracy of the empirical relationships used to calculate the module's key parameters such as the effective Seebeck coefficient (SM), Electrical Resistance (RM), and Thermal Conductance (KM) in Equations 16 through Equation 20.

## 5. CONCLUSIONS

During this study, the behavior of PV-Thermal and thermoelectric generator were presented. In addition, the characteristics nanofluids AI2O3, CuO, Fe304 and SIO2 circulating in PV-Thermal solar panel and driving the thermoelectric generator were also presented. Furthermore, the key parameters of the thermoelectric generator have been modeled and integrated into the present model. Finally, the results were discussed and compared to experimental data.

The model in this study was established after the mass and energy conservation equations coupled with the heat transfer equations nanofluids; AI2O3, CuO, Fe304 and SIO2 and the key parameters of the thermoelectric generator. The concentrations of the nanoparticles vary from 1% through 50%. Thermodynamic, thermophysical and heat transfer properties of the nanofluids were obtained from the available data in the literature. The resulted presented hereby showed that higher the nanoparticles concentration increase the thermal heat released by the PV-Th panel, and the higher the power generated by the thermoelectric device. Furthermore, it was also shown that higher nanoparticles concentration increased the heat transfer properties heat transferred to the nanofluid, this increased the thermoelectric generator device efficiency and the hybrid system efficiency. In addition, numerical results also showed that the nanofluid Fe304 has the highest thermal heat transfer to HTF and the highest thermoelectric generator and hybrid efficiencies.

Finally, the numerical model predicted results fairly compared with the data reported in the literature on the PV solar panels and TEG.

### NOMENCLATURE

$A_{Panel,}$ Area of solar panel (m^2)

$A_{f,}$ Flow area (m^2)

$C_{pw,}$ Specific heat of water (kJ/(kg K))

G, Radiation (W/m^2)

h, Heat transfer coefficient

$K_{w,}$ Thermal conductivity of water (kJ/(ms°C))

l, Tube length (m)

$m_w$, Water mass flow rate (kg/s)

N: number finite different element (N: 1-12)

$Q_{thermal}$, Heat (kJ)

R, Tube radius (m)

$T_{(water]\_m}$ ), Temperature of HTF at "m" element (°C)

**Greek**

$\rho_w$, Density of water flow (kg/m^3)

μ, Water viscosity (m^2/s)

**Subscripts**

| | |
|---|---|
| Qth | Thermal heat |
| pv | PV solar panel |
| nf | Nanofluid |
| sh | Hybrid system |
| w | HTF |
| Tub | Tube |
| w | Water |

**Funding:** This study is funded by the Catholic University of Cuenca.
**Competing Interests:** The authors declare that they have no competing interests.
**Contributors/Acknowledgement:** Both authors contributed equally to the conception and design of the study.

## REFERENCES

Al Musleh, M., T. Evangelia, J. Lynne and J. David, 2017. Thermoelectric generator experimental performance testing for wireless sensor network application in smart buildings. MATEC Web of Conferences, 120: 08003.

Allen, C., 2015. Magnetic field enhancement thermal conductivity analysis of magnetic nanofluids. MScE, University of Texas at Arlington.

Azo Material, 2004. Available from http://www.azom.com/properties.aspx.

Bachock, N. and I. Pop, 2012. Flow and heat transfer characteristics on a moving plate in a nanofluid. International Journal of Heat and Mass Transfer, 55: 642-648.

Beeby, S. and N. White, 2010. Energy harvesting for autonomous systems. Artech House.

Brenner, H., D.A. Edwards and D.T. Wasan, 1993. Interfacial transport process and rheology. New York, USA: Butterworth.

Buist, R., 1995. Calculation of peltier device performance. CRC Handbook of Thermoelectrics: 143-155.

Chaudhari, K.S. and P.V. Walke, 2014. Applications of nanofluid in solar energy- a review. International Journal of Engineering Research & Technology, 3(3): 460-463.

Chen, M., L.A. Rosendahl, T.J. Condra and J.K. Pedersen, 2009. Numerical modeling of thermoelectric generators with varing material properties in a circuit simulator. IEEE Transactions on Energy Conversion, 24(1): 112-124.Available at: https://doi.org/10.1109/tec.2008.2005310.

Choi, U.S., 1995. Enhancing thermal conductivity of fluids with nanoparticles. ASME FED, 231: 99-103.

CRC, 1995. CRC handbook of thermoelectrics, introduction, Edited by D.M. Rowe. CRC Press.

Dalola, S., M. Ferrari, V. Ferrari, D.M. Guizzetti and A. Taroni, 2008. Characterization of thermoelectric modules for powering autonomous sensors. IEEE Transaction on Instrumentation and Measurement, 58(1): 99-107.Available at: https://doi.org/10.1109/tim.2008.928405.

De Baetselier, E., G. De Mey and A. Kos, 1995a. Thermal image generator as a vision prosthesis for the blind. MST Poland News, 3(7): 3-5.

De Baetselier, E., W. Goedertier and G. De Mey, 1995b. Thermoregulation of IC's with high power dissipation. Proceedings of the 10th European hybrid Microelectronics Conference,Copenhagen, Denmark, May 1995, ISHM. pp: 425-439.

DiSalvo, F.J., 1999. Thermoelectric cooling and power generation. Science, 285(5428): 703-706.Available at: https://doi.org/10.1126/science.285.5428.703.

Dziurdzia, P. and A. Kos, 1999. Electrothermal macromodel of active heat sink for cooling process simulation. Proc. of the 5-th International Workshop on Thermal Investigation of Ics and Microstructures, Roma, Italy, October 4-6, 1999. Sustainable Energy Harvesting Technologies – Past, Present and Future 128. pp: 76-81.

Dziurdzia, P. and A. Kos, 2000. High efficiency active cooling system. Proceeding of the XVIth Annual IEEE Semiconductor Thermal Measurement and Management Symposium SEMITHERM, San Jose, USA, 21-23 March 2000. pp: 19-26.

Faragali, H., M., F.H. Fahmy and M.A. Hassan, 2008. A simulation model for predicting the performance of PV/wind- powered geothermal space heating system in Egypt. The Online Journal on Electronics and Electrical Engineering, 2(4).

Faruk, Y., L.C. Keith and C. Bill, 2013. An applied compares study: Solar energy vs. Thermoelectric energy, Paper ID:#5845. 120th ASEE Annual & Exposition.

Freunek, M., M. Müller, T. Ungan, W. Walker and L.M. Reindl, 2009. New physical model for thermoelectric generators. Journal of Electronic Materials, 38(7): 1214-1220.Available at: https://doi.org/10.1007/s11664-009-0665-y.

Good, C., J. Chen, Y. Dai and A.G. Hestnes, 2015. Hybrid photovoltaic-thermal system: A review. Energie Procedia, 70: 683-690.

Hashim, H., J. Bomphrey and G. Min, 2016. Model for geometry optimisation of thermoelectric devices in a hybrid PV/TE system. Renewable Energy, 87(P1): 458-463.Available at: https://doi.org/10.1016/j.renene.2015.10.029.

History, 1920. History of thermoelectrics, custom thermoelectric. California Institute of Trchnology, Caltech Material Science, 1820-1920.

Jatin, P., M. Patel, J. Patel and H. Modi, 2016. Improvement in the COP of thermoelectric cooler. International Journal of Scientific & Technology Research, 5(05): 73-76.

Jeffrey, S.G. and S.T. Eric, 2008. Complex thermoelectric materials. Nature Material, 7: 105-114.

Kakaç, S. and A. Pramuanjaroenkij, 2009. Review of convective heat transfer enhancement with nanofluids. International Journal of Heat and Mass Transfer, 52(13-14): 3187-3196.Available at: https://doi.org/10.1016/j.ijheatmasstransfer.2009.02.006.

Kasaeian, A., A.T. Eshghi and M. Sameti, 2015. A review on the applications of nanofluids in solar energy systems. Renewable and Sustainable Energy Reviews, 43(C): 584-598.Available at: https://doi.org/10.1016/j.rser.2014.11.020.

Khullar, V., H. Tyagi, P.E. Phelan, T.P. Otanicar, H. Singh and R.A. Taylor, 2013. Solar energy harvesting using nanofluids-based concentrating solar collector. Journal of Nanotechnology in Engineering and Medicine, 3(3): 031003.

Liang, R., J. Zhang and C. Zhou, 2015. Dynamic simulation of a novel solar heating system based on hybrid photovoltaic/thermal collectors (PVT). Procedia Engineering, 121: 675-683.Available at: https://doi.org/10.1016/j.proeng.2015.09.001.

Maiga, S.E.B., S.J. Palm, C.T. Nguyen, G. Roy and N. Galanis, 2005. Heat transfer enhancement by using nanofluids in forced convection flows. International Journal of Heat and Fluid Flow, 26(4): 530-546.

Nerella, S., N. Sudheer and P. Bhramara, 2014. Enhancement of heat transfer by nanofluids in solar collectors. International Journal of Engineering and Technology, 3: 115-120.

Patrizia, R., D.G. Pedro, C.G. Luís and A. David, 2011. The experimental results analysis of the energy conversion efficiency of thermoelectric generators. Renewable Energies and Power Quality Journal, 1(9): 278-282.Available at: https://doi.org/10.24084/repqj09.312.

Pei, G., F. Huide, Z. Tao and J. Jie, 2011. A numerical and experimental study on a heat pipe PV/T system. Solar Energy, 85(5): 911-921.Available at: https://doi.org/10.1016/j.solener.2011.02.006.

Piotr, D., 2014. Modeling and simulation of thermoelectric energy harvesting processes. AGH University of Science and Technology in Cracow Poland.

Rowe, D.M., 1999. Thermoelectrics, an environmentally-friendly source of electrical power. Renewable Energy, 16(1-4): 1251-1256.Available at: https://doi.org/10.1016/s0960-1481(98)00512-6.

Sagadevan, S., 2015. A review of role of nanofuids for solar energy applications. American Journal of Nano Research and Applications, 3(3): 53-61.

Saleh, A.M., 2012. Modeling of flat-plate solar collector operation in transient states. MsE Thesis, Purdue University, Fort Wayne, Indiana.

Sami, S., 2018. Enhancement of performance of thermal solar collectors using nanofluids. International Journal of Energy and Power Engineering, 7(1-1): 1-8.

Sami, S., 2018. Impact of magnetic field on the enhancement of performance of thermal solar collectors using nanofluids. International Journal of Ambient Energy: 1-10.Available at: https://doi.org/10.1080/01430750.2018.1437561.

Sami, S., 2018. Modeling and simulation of a novel combined solar photovoltaic-thermal panel and heat pump hybrid system. Clean Technologies, 1(1): 89-113.Available at: https://doi.org/10.3390/cleantechnol1010007.

Sami, S. and C. Campoverde, 2018. Dynamic simulation and modeling of a novel combined hybrid photovoltaic-thermal panel hybrid system. International Journal of Sustainable Energy and Environmental Research, 7(1): 1-23.Available at: https://doi.org/10.18488/journal.13.2017.71.1.23.

Sami, S. and E. Marin, 2017. A numerical model for predicting performance of solar photovoltaic, biomass and CHP hybrid system for electricity generation. International Journal of Engineering Sciences & Research Technology, 4(1): 1- 22.

Sami, S. and E. Marin, 2017. Simulation of solar photovoltaic, biomass gas turbine and district heating hybrid system. International Journal of Sustainable Energy and Environmental Research, 6(1): 9-26.Available at: https://doi.org/10.18488/journal.13/2017.6.1/13.1.9.26.

Sami, S. and E. Marin, 2018. Dynamic modeling and simulation of hybrid solar photovoltaic and PEMFC fuel power system. RA Journal of Applied Research, 4(5): 1664-1683.Available at: https://doi.org/10.31142/rajar/v4i5.02.

Sami, S. and J. Rivera, 2017. A predictive numerical model for analyzing performance of solar photovoltaic, geothermal hybrid system for electricity generation and district heating. Science Journal Energy Engineering, 5(1): 13-30.Available at: https://doi.org/10.11648/j.sjee.20170501.12.

Sharma, K.V., A. Suleiman, H.S.B. Hassan and G. Hegde, 2017. Considerations on the thermophysical properties of nanofluids. In Engineering Applications of Nanotechnology. Springer, Cham. pp: 33-70.

Snyder, G. and T. Ursell, 2003. Thermoelectric efficiency and compatibility. Physical Review Letters, 91(14): 148301-148301.Available at: https://doi.org/10.1103/physrevlett.91.148301.

Taylor, R.A., P.E. Phelan, T.P. Otanicar, C.A. Walker, M. Nguyen, S. Trimble and R. Prasher, 2011. Applicability of nanofluids in high flux solar collectors. Journal of Renewable and Sustainable Energy, 3(2): 023104.Available at: https://doi.org/10.1063/1.3571565.

The Science of Thermoelectric Materials, 2019. The seebeck effect, thermoelectric caltech materials science, thermoelectrics. [Accessed January 3, 2013].

Warren, M.R., 2019. Thermal radiaton: Planck's law. Heat and mass transfer laboratory. Available from http://ocw.mit.edu/courses/mechanical-engineering/2-997-direct-solar-thermal-to-electricalenergy-conversion-technologies-fall-2009/audio-lectures/MIT2_997F09_lec02.pdf [Accessed January 3, 2013].